July 21, 2000

Dr. Harry Spilker
Department Head, Special Projects
Gesellschaft für Nuklear-Behälter mbH
Hollestaße 7A
D-45127 Essen
GERMANY

Dear Dr. Spilker:

Thank you for taking time out of your busy schedule to talk with U.S. Nuclear Regulatory Commission staff after your meeting on the Castor X/33 application. In our discussions, you indicated that you possess significant amount of data on creep of zirconium based cladding material. In the United States, similar data are obtained by the fuel fabricators and programs are being initiated to obtain more data on spent fuel with burnups exceeding 45 GWd/MTU.

As you requested, I am enclosing a contractor report that was prepared to support our review and approval of the storage of high burnup fuel in the FuelSolutions storage cask. The WCAP-15168 that is referenced in this contract report is proprietary, so we will not be able to share that data with you. However, the WCAP-15168 report relies heavily on references which are publically available including research conducted by the Japanese (e.g., Y.K. Matsuo and M. Mayuzumi) and some of your colleagues (e.g., G. Kaspar, M. Peehs, G. Porsch, and H.J. Romeiser).

Next year, I plan to travel to Europe to present the U.S. Nuclear Regulatory Commission position on dry cask storage and transportation of high burnup fuel. During that trip, I would like to accept your and Dr. Schmidt's kind invitation to meet with you, discuss the high burnup fuel data, and to observe your storage casks and welding techniques to be used for the Castor X/33.

I look forward to meeting with you next summer to discuss the behavior of zirconium-based cladding materials under dry storage conditions in more detail.

Sincerely,
/S/
Kimberly Ann Gruss
Materials Engineer
Spent Fuel Project Office
Office of Nuclear Material Safety
and Safeguards

Enclosure - Letter dated 3/23/2000
w/Attachment - Technical Evaluation Report of WCAP-15168

cc: Dr. Paul Schmidt, Project Manager
Gesellschaft für Nuklear-Behälter mbH

DISTRIBUTION:
SFPO r/f Public SGagner, OPA JGuttman CBrown

G:\KIMGRUSS\spilker_letter.wpd *SEE PREVIOUS CONCURRENCE

OFC:	SFPO*	E	SFPO*		SFPO		SFPO	
NAME:	KGruss Kag		EEaston		WHodges		EWBrach	
DATE:	7/21/00		7/21/00		7/21/00		7/21/00	

OFFICIAL RECORD COPY

UNITED STATES
NUCLEAR REGULATORY COMMISSION
WASHINGTON, D.C. 20555-0001

July 21, 2000

Dr. Harry Spilker
Department Head, Special Projects
Gesellschaft für Nuklear-Behälter mbH
Hollestaße 7A
D-45127 Essen
GERMANY

Dear Dr. Spilker:

Thank you for taking time out of your busy schedule to talk with U.S. Nuclear Regulatory Commission staff after your meeting on the Castor X/33 application. In our discussions, you indicated that you possess significant amount of data on creep of zirconium based cladding material. In the United States, similar data are obtained by the fuel fabricators and programs are being initiated to obtain more data on spent fuel with burnups exceeding 45 GWd/MTU.

As you requested, I am enclosing a contractor report that was prepared to support our review and approval of the storage of high burnup fuel in the FuelSolutions storage cask. The WCAP-15168 that is referenced in this contract report is proprietary, so we will not be able to share that data with you. However, the WCAP-15168 report relies heavily on references which are publically available including research conducted by the Japanese (e.g., Y.K. Matsuo and M. Mayuzumi) and some of your colleagues (e.g., G. Kaspar, M. Peehs, G. Porsch, and H.J. Romeiser).

Next year, I plan to travel to Europe to present the U.S. Nuclear Regulatory Commission position on dry cask storage and transportation of high burnup fuel. During that trip, I would like to accept your and Dr. Schmidt's kind invitation to meet with you, discuss the high burnup fuel data, and to observe your storage casks and welding techniques to be used for the Castor X/33.

I look forward to meeting with you next summer to discuss the behavior of zirconium-based cladding materials under dry storage conditions in more detail.

Sincerely,

Kimberly Ann Gruss

Kimberly Ann Gruss
Materials Engineer
Spent Fuel Project Office
Office of Nuclear Material Safety
and Safeguards

Enclosure - Letter dated 3/23/2000
w/Attachment - Technical Evaluation Report of WCAP-15168

cc: Dr. Paul Schmidt, Project Manager
Gesellschaft für Nuklear-Behälter mbH

March 23, 2000

MEMORANDUM TO: M. Wayne Hodges, Deputy Director
Technical Review Directorate
Spent Fuel Project Office
Office of Nuclear Material Safety
and Safeguards

FROM: Kimberly Gruss, Materials Engineer
Technical Review Section A (Original Signed by:)
Spent Fuel Project Office
Office of Nuclear Material Safety
and Safeguards

SUBJECT: PNNL TECHNICAL EVALUATION REPORT ON CLADDING BEHAVIOR FOR HIGH BURNUP FUELS

In support of the staff's evaluation of the BNFL Fuel Solutions Corporation (BFS) Wesflex Spent Nuclear Fuel Dry Storage System (Docket Number 72-1026), the staff contracted with PNNL (Job Code Number J5167, Task-8) for technical assistance to assess the long-term cladding behavior of high burnup fuels. The analyses prepared by PNNL were used in the staff's review of BFS' proposed method for establishing maximum allowable cladding temperature limits for high burnup nuclear fuel rods. Attached is a copy of the PNNL report, "Technical Evaluation Report of WCAP-15168 (Dry Storage of High Burnup Spent Nuclear Fuel)," that we considered in our evaluation of the applicant's submittal.

Docket No.: 72-1026

Attachment: Technical Evaluation Report of WCAP-15168

Non-Proprietary

Technical Evaluation Report of WCAP-15168 (Dry Storage of High Burnup Spent Nuclear Fuel)

E. R. Gilbert
C. E. Beyer
E. P. Simonen

February 2000

TABLE OF CONTENTS

1.0 Introduction 5

2.0 Assessment of BFS/Spilker Approach to Calculating Temperature Limits 5

2.1 BFS Creep Methodology 5
2.2 Creep Reduction Factor 7
2.3 Voids and Grain Boundary Cavitation 9
2.4 Monkman-Grant Correlation for Zry-4 12
2.5 Comparison of Spilker/BFS and CSFM Creep Predictions 12

3.0 Assessment of the 1% Strain Limit 14

4.0 Assessment of Maximum Rod Pressure 17

5.0 Major Issues Identified 18

5.1 Variability in Creep for different Lots of Zr Alloys 18
5.2 Embrittlement of Hydride Enriched Rim for Cladding with High Corrosion 19
5.3 Early BWR Fuel Rods with Nodular Corrosion 19
5.4 Summary of Issues 19

6.0 Conclusions 20

7.0 Recommendations for Additional Investigations 22

8.0 Bibliography 23

TABLES & FIGURES

Table 1. Effect of Irradiation on Creep Reduction Factor 9

Table 2. Comparison of Temperature Limits for BFS 13

Figure 1. Evaluation of Time Exponents for Unirradiated and Irradiated FRG-2 Cladding Creep Strain at 395°C and 86 MPa 28

Figure 2. Effect of Stress on Creep Reduction Factor for Irradiated Zry-4 29

Figure 3. Comparison of Creep Strains for Type I Cladding with Creep for Sandvik Cladding 30

Figure 4. Deleted - Proprietary Information 31

Figure 5. Scanning Electron Micrograph showing Cavities in Zry-4 Specimens Crept for 240 h to 3 % Strain at 375°C and 132 MPa. No cavities were found in unstrained specimens (Keusseyan et al. 1979). The number density of grain boundary cavities in Zry-2 specimens increased with increasing creep strain (Keusseyan and Li 1981). 32

Figure 6. Radiation-Induced Cavities in Zr Alloys [ORR] 33

Figure 7. TEM Micrograph of Zry-4 Showing Voids "v" and Cavities "c" after Irradiation in EBR-II at 381C and 1.4 to 6.3 x 10^{21} n/cm2 E>1 MeV (Adamson et al. 1982) 34

Figure 8. TEM Micrograph of Irradiated Zry-4 Showing Grain Boundary Cavitation after Irradiation in EBR-II at 381°C and 1.4 to 6.3 x 10^{21} n/cm^2 E>1 MeV (Adamson et al. 1982) 35

Figure 9. Cavities in Zr After Irradiation in EBR-II (Griffiths et al. 1987) at: 36

Figure 10. Cavity in Zr Irradiated in DFR at 452°C, 1.7 x 10^{21} n/cm^2 E>1 MeV (Griffiths et al. 1994) 37

Figure 11. Tensile Test Fracture in 30 GWd/MTU H.B. Robinson Zry-4 Cladding by Cavitation (Bauer and Lowry 1978) 38

Figure 12. Fracture in Zry-4 by Nucleation, Growth, and Coalescence of Voids (Bai et al. 1994) 39

Figure 13. Fracture in Stainless Steel by Nucleation, Growth, and Coalescence of Voids (Angeliu and Was 1994) 40

Figure 14. Fracture in Zry by Nucleation, Growth, and Coalescence of Voids (Puls 1998) 41

Figure 15. Comparison of the Temperature Dependence for the Spilker et al. (1997) Equation and the CSFM Methodology (Levy et al. 1987) 42

Figure 16. Comparison of the Stress Dependence for the Spilker et al. (1997) Equation and the CSFM Methodology (Levy et al. 1987) 43

Figure 17. Comparison of Predicted Strain vs Time for the Spilker et al. (1997) Equation and the CSFM Methodology (Levy et al. 1987); Temperature and Stress Transients are for Zion Example 1 with the BFS Cooling Curves for 9.1-Year-Old SNF During Cask Storage 44

Figure 18. Comparison of Calculated Damage Fraction and Strain Fraction versus Initial Maximum Cladding Temperature with No Creep Reduction as Calculated by the CSFM Methodology for an Initial Cladding Stress of 122 MPa and the BFS Cooling Curves in Figure 4-16, page 4-31 from WCAP-15168 45

Figure 19. Comparison of Calculated Damage Fraction and Strain Fraction versus Initial Maximum Cladding Temperature with a 50% Creep Reduction Factor as Calculated by the CSFM Methodology for an Initial Cladding Stress of 122 MPa and the BFS Cooling Curves in Figure 4-16, page 4-31 from WCAP-15168 46

Figure 20. Effect of Creep Reduction Factor on Temperature Limits for BFS 1% Strain Limit Method and the CSFM Damage Limit Method 47

Figure 21. Effect of Stress on Temperature Limits Showing the BFS/Spilker/2 Correlation Is Conservative Compared to the CSFM Methodology for Stresses above 80 MPa. (Note: 80 MPa is the lower limit of applicability for the Spilker Equation.) 48

1.0 Introduction

BNFL Fuel Solutions (BFS) has submitted to the U.S. Nuclear Regulatory Commission (NRC) a topical report, entitled "Dry Storage of High Burnup Spent Nuclear Fuel," WCAP-15168, for review and approval. This report provides the licensing basis for BFS to determine allowable peak cladding temperatures for their dry storage casks. This submittal further requests application of this methodology up to rod-average burnup levels of 60 GWd/MTU.

Pacific Northwest National Laboratory (PNNL) has acted as a consultant to the NRC in this review. The following is a summary of PNNL's review of the topical report and BFSs responses to request for additional information (RAI) as of December 31, 1999.

2.0 Assessment of BFS/Spilker Approach to Calculating Temperature Limits

2.1 BFS Creep Methodology

Complete equations for creep in materials usually consist of four components, each progressively transitions into the following stages:

- instantaneous - plastic deformation that results as the load is applied
- primary creep stage - creep that decreases in rate until it saturates
- secondary creep stage (steady state) - creep that progresses at a constant rate, i.e., is steady with time
- tertiary stage creep - creep that accelerates toward fracture.

Depending on the material and conditions all four stages are not always observed.

The time dependence for the Spilker et al. (1997) equation applied to creep in SNF cladding during dry storage is similar to a formulation by Andrade (1910, 1914) for the primary creep stage. Except for very brittle materials, it is uncommon to apply only primary stage creep, because it does not include components for the secondary and tertiary stages that describe the useful lifetime for ductile materials and the failure behavior. Primary creep formations are most useful for describing small initial strains that result early in life, but additional creep terms are needed for modeling the failure thresholds. BFS applies a primary creep formulation to a limiting strain of 1%. In contrast, Limback and Andersson (1996) show that primary creep saturates at strains less than 0.3% for temperatures and stresses corresponding to dry storage of SNF. Above 0.3% strain, Limback and Andersson consider Zry-4 creep to be in the steady-state mode.

A non-conservative feature of the Spilker equation is that the creep rate is predicted to decrease during cask storage not only because of the decreasing pressure (hoop stress) and declining temperature associated with the decreasing decay heat, but also because it fails to transition from saturated-transient to steady-state creep. Creep data and creep

mechanistic creep models for Zr alloys clearly show that for SNF dry storage conditions the transient creep stage saturates before the 1% strain limit used by BFS is reached. Therefore the creep strain may be larger than predicted by the Spilker correlation. Although the Spilker correlation bounds the total creep strains achieved during testing of Type 1 cladding out to 10,000 hours, the slopes on plots of log-strain vs log-time defined by the data points beyond 2,000 hours are steeper than indicated by the equation. These steeper slopes indicate that the transient Spilker correlation is under predicting the creep trends for periods beyond 2,000 hours. In other words, the Spilker correlation over predicts the transient-strain behavior of the Type 1 cladding up to 2,000 hours, and under predicts the steady-state creep behavior beyond 2,000 hours. A graphical comparison by Spilker et al. (1997) for the Spilker equation and Type I data show that at 375°C the data catch up and intersect the equation at 10,000 hours. This problem becomes more serious for predicting longer-term storage temperature limits.

The temperature and stress dependencies for creep by the Spilker et. al. equation are contained in the time exponent. The terms for temperature and stress were developed for creep of unirradiated Zry-4 with polynomial equations to describe the strain-time behavior for different temperatures and stresses. Polynomial equations are effective for interpolation within the range of test variables, but can be unwieldy if extrapolated beyond the range of test conditions. Therefore caution should be taken to validate significant extrapolation of the Spilker et al. equation beyond the temperature and stress range of the data. Spilker et al. appropriately limit application of their equation to the temperature and stress ranges of the data for unirradiated Type 1 Zry-4. However, even though the equation predicts a continuously declining strain rate, and does not transition into steady state, no limit is cited for extrapolation in time.

The CSFM methodology models metallurgical changes due to temperature-time thermal exposure. The model is based on unirradiated data and needs to be updated to benefit from recently published data. The Spilker correlation does not address metallurgical changes such as annealing that may occur during exposure to elevated temperature.

Another limitation of the Spilker equation is that the total ranges of temperatures, stresses, and storage periods for SNF cladding expected during dry storage extend beyond the temperature, stress, and time ranges of applicability for the Spilker formulation. Extraordinarily high values of allowable temperature resulted from calculations by BFS for Big Rock Point SNF, which were outside the range of applicability for the Spilker correlation.

The BFS approach utilizes the reduction in creep rate with time predicted by the primary creep characteristics of the Spilker equation to prevent SNF cladding from reaching the 1% strain limit during dry storage. Verification of the primary nature of creep in SNF cladding is based on creep tests with irradiated FRG-2 cladding that were terminated at 8,000 hours and prior to achieving 0.3% strain. Examination of these results on plots of log-strain versus log-time in Figure 1 resulted in a slope larger than unity, indicating that transient creep was saturated. The data-based creep model by Limback and Andersson (1996) for Zry-2 and Zry-4 show that at 80 MPa stress the saturated primary creep strain

increases from <0.1% at 330°C to <0.3% at 385°C. The exponent on time beyond these creep strains indicates that secondary creep (steady-state) is the mode for further creep. Post-irradiation creep data at 300°C and 310 MPa by Fidleris (1979) show the onset of secondary creep at a strain of ~0.3%. Inspection of creep data by Spilker et al. (1997) show that for periods beyond 2,000 hours, the slopes for the data on log-strain vs log-time plots exceed those for the equation.

2.2 Creep Reduction Factor

BFS initially proposed that the creep strain for irradiated cladding was a factor of 20 less than for unirradiated Zry-4 cladding; however, a questionable interpretation of data was presented to justify a factor of 20. As a result of NRC RAIs, BFS reduced the factor of 20 to a factor of 10. Spilker et al. (1997) applied a creep reduction factor of unity for their development of a temperature limit for high burnup SNF.

Because of lattice defects produced by neutron bombardment during irradiation, cladding creep is reduced and cladding burst and tensile strengths are increased for temperatures encountered by SNF in dry cask storage (200 to 400°C) for high stresses >~300 MPa. Figure 2 shows that creep reduction factors of ~30 to ~55 are consistent with stresses of ~400 MPa (Schaffler-Le Pichon et al. 1997, Hoppe 1991). Creep reduction factors of ~10 are consistent with a stress of 310 MPa (Fidleris 1979, Schaffler-Le Pichon et al. 1997). However, for low stresses corresponding to peak SNF cladding stresses (<~140 MPa), the creep reduction is much less. Two data sets that may be used to evaluate the creep reduction factor at low stresses due to irradiation are the creep data for FRG-2 data by Kaspar et al. (1985) and the KWO SNF cladding data by Peehs et al. (1983). A benefit of these data is that they are for the same source of Zircaloy-4 and the results are not confused by lot-to-lot or vendor-to-vendor variations for unirradiated Zry-4.

Typical cladding strains for FRG-2 unirradiated and irradiated cladding during creep at 395°C and 86 MPa stress are plotted in Figure 1. During the first 1,000 hours, the unirradiated cladding deformed to ~0.1% strain, while the majority of the irradiated cladding exhibited a factor of 10 or more lower strain. The initial creep rate for the unirradiated cladding was low because the initial test temperature was lower during the first 1000 hours.

During the first 1,000 hours, creep was restrained (nearly zero) in the irradiated cladding by the lower initial temperature and by the internal stresses caused by residual anisotropic growth strains generated during irradiation. Relaxation of these residual stresses during the post-irradiation creep test requires ~1,000 h. After the 1,000-hour induction period, the residual stresses had relaxed, and the creep strains became measurable.

The average creep reduction factor after 6 months (4380 hours) estimated by comparing the creep in the KWO SNF unirradiated plenum cladding with the creep in the range of maximum burnup appears to be <4. The ratio of the cladding strain for the unirradiated to the irradiated FRG-2 cladding after 4380 hours is also ~4.

On logarithmic scales, the creep reduction factor, taken as the ratio of strains for unirradiated and irradiated cladding in Figure 1, appears to decrease with increasing test period such that a factor of ~5 at 2000 hours decreases to ~2 at 8000 hours. These results are summarized in Table 1. Extrapolation of the curves in Figure 1 suggest that the irradiated creep curves may converge with the unirradiated at long times, and the creep reduction factor may by only unity in less than 20,000 hours of test time.

As shown in Table 1, comparison of the creep rates for the unirradiated and irradiated FRG-2 data from Table 11 in Kaspar et al. (1985) between 4,000 and 8,000 hours resulted in an average creep rate reduction factor of ~1.1. This is consistent with the observation in Figure 1 that the unirradiated and irradiated creep curves are converging for long time periods. This result indicates that the apparent creep reduction factor is primarily a result of a lower initial test temperature and the residual stresses in the irradiated cladding at the onset of creep. The standard deviation on the data are larger than the difference between the unirradiated and irradiated FRG-2 data. Therefore, there is no statistical difference in the creep rates. These results are summarized in Table 1. These results and other consideration lead to the conclusion that the creep reduction factor due to pre-irradiation is <2. This reduction appears to be caused primarily by the effect of the residual stresses generated during pre-irradiation

A variation of a factor of 10 for the creep strains, measured for the Types I, II, III, IV, V, VI, and FRG-2 unirradiated cladding (Spilker et al. 1997), has been used by BFS to validate a creep reduction factor of 10. This variation in creep behavior for different lots of cladding may result from different, compositions and thermal-mechanical processing effects on texture, grain size, and microstructure. These variations are not precluded by ASTM B353 to which Zry-4 tubing or ASTM B811 to which cladding is specified and procured. Prasad et al. (1988) showed that the creep mechanisms in the temperature range of 510 to 720°C could be changed by increasing the average grain diameter from 12 to 17 μm and by changing the characteristics of the precipitates at grain boundaries. The Spilker equation bounds the Type I cladding, which has the least resistance to creep, but the data trends indicate that the equation may not be bounding beyond the 10,000 hour range of the Type I cladding data.

Creep strains for Sandvik (Limback and Andersson 1996) cladding are compared with Type I cladding in Figure 3. The strains for Sandvik SRA Zry-4 cladding in Figure 3 are based on normalization of their data for SRA Zry-2. The results for Type I cladding in Figure 3 are based on interpolation of the Type I cladding data by Spilker et al. (1997). A proprietary creep model for Westinghouse unirradiated cladding (Foster 1991) has also been compared to the BFS creep model. The results show that the BFS creep correlation which normalizes the Spilker creep equation by a creep reduction factor of 10 to match the characteristics of the creep-resistant FRG-2 cladding significantly under predicts creep strains for Sandvik and Westinghouse type cladding under the temperature conditions proposed for the WESFLEX Storage Systems.

Table 1. Effect of Irradiation on Creep Reduction Factor at 86 MPa Cladding Stress					
Creep Results for Unirradiated FRG-2 Zry-4 Cladding					
Test ID	Strain Rate From 4000 to 8000 h, 10^{-5} %/h	Strain at 2000 h, %	Strain at 8000 h, %	Time Exponent, m	R^2
2150B	4.25	0.18	0.530	0.83	0.97
2151B	3.00	0.255	0.555	0.74	0.92
2160A	3.38	0.135	0.395	0.69	0.98
2161A	1.75	0.23	0.490	0.64	0.95
Average	3.1	0.2	0.49	0.73	0.96
Creep Results for Irradiated FRG-2 Zry-4 Cladding					
2117A	3.63	-	0.212	1.5	0.99
8877B	3.00	0.025	0.27	1.61	0.87
2103B	3.25	0.01	0.26	2.2	0.88
2104B	2.25	0.005	0.26	2.54	0.75
2139B	2.75	0.1	0.245	0.65	0.95
2140B	2.38	0.15	0.26	0.41	0.90
2133B	2.88	0.02	0.26	1.2	0.78
2134B	2.50	0.02	0.255	1.3	0.81
Average	2.8	0.041	0.221	1.4	0.87
Creep Reduction Factor	1.1	5	2	-	-

BFS has incorrectly associated a creep reduction factor of 10 with the factor of 10 reduction in creep strain ductility applied by the CSFM model. These two factors are similar only in value. They have opposite effects on the conservatism for predicting cask storage temperature limits. For example, the BFS factor of 10 reduces creep by a factor of 10, which increases maximum cask storage temperature limits. The CSFM factor of 10 reduction in allowable strain (from unirradiated to irradiated Zr-4) will lower maximum cask storage limits, which is the opposite effect of the BFS factor of 10 on creep rate. A creep strain ductility reduction by a factor of 10 in the CSFM methodology reduces the temperature limit, and corresponds, in principle, to the BFS fracture strain limit of 1%.

2.3 Voids and Grain Boundary Cavitation

The deformation of even super-plastic Zr alloys is limited by the tendency to develop intergranular cavities and cavitation (Shukla et al. 1999, Hayes et al. 1999, Keusseyan et al. 1979, Keusseyan and Li 1981, Kearns et al. 1976, Bocek et al. 1977). Cavities are generally recognized to be caused by deformation incompatibility at grain boundary precipitates, at steps, and at corners resulting from grain boundary sliding (Toscano and Bocek 1981, Bocek 1985).

BFS concludes that unlike other metals and alloys, SNF Zry-4 cladding is immune to void formation or grain boundary cavitation. To prove this immunity, they cite Pescatori and Cowgill (1994) who reviewed results for investigations conducted in the fracture regimes not controlled by grain boundary cavitation, but by transgranular and triple point cracking. After examining the evidence in the regions where fracture is not controlled by cavitation, they concluded that cavitation was not relevant to Zr alloys. They disregarded a study in which grain boundary cavities were reported by Keusseyan et al. (1979) and concluded that cavitation is not relevant for Zr alloys. BFS states concurrence that grain boundary cavitation is not a failure mechanisms for Zr alloys. Work by Keusseyan et al. (1979) showed cavities in Zry-4 specimens crept for 240 hours to 3 % strain at 375°C and 132 MPa, but no cavities were found in unstrained specimens (Keusseyan et al. 1979). A typical scanning electron micrograph is shown in Figure 5. The number density of grain boundary cavities in Zry-2 specimens increased with increasing creep strain (Keusseyan and Li 1981).

As presented below, numerous publications have demonstrated that cavities and grain boundary cavitation are not limited to non-Zr alloys, but are also found in Zr and Zr alloys in the temperature and neutron fluence range of high-burnup LWR SNF cladding. After irradiation at 400°C in the Oak Ridge Reactor to neutron fluences of 0.7 to 1.2×10^{21} n/cm^2 (E>0.1 MeV) Gilbert et al. (1979) demonstrated the presence of cavities in annealed crystal-bar Zr, annealed Zry-2, and annealed Zr-2.5 wt% Nb after irradiation at 675°C. An example of cavities from their investigation is shown in Figure 6.

Adamson et al. (1982) show voids and grain boundary cavitation for Zircaloy-4 after irradiation in the Experimental Breeder Reactor II to neutron fluences of 1.4 to 6.3×10^{21} n/cm^2 (E>0.1 MeV) at 375°C. Examples of cavities from their investigation are shown in Figures 7 and 8.

Cavities are reported in crystal-bar, sponge Zr, and in Zr alloys following irradiation in EBR-II up to 6×10^{21} n/cm^2 (E>1 MeV) at 371 to 437°C (Griffiths, et al. 1987). Griffiths et al. (1988) found cavities, mostly adjacent to grain boundaries, in Zr and Zry-2 following irradiation in EBR-II at ~390 to 440°C for neutron fluences up to 1.5×10^{22} n/cm^2 (E>1MeV). An example of cavities from their investigation is shown in Figure 9. Cavities are also reported by Griffiths et al. (1994) in Zr irradiated in the Dounreay Fast Reactor to 0.2×10^{21} n/cm^2 (E>1 MeV) at ~470°C and 1.7×10^{21} n/cm^2 (E>1 MeV) at ~452°C (Figure 10) and voids by Holt et al. (1982) in annealed Zry-2 following irradiation in EBR-II to a neutron fluence of 6.3×10^{21} n/cm^2 (E>0.1 MeV) at 417°C.

Griffiths et al. (1993) evaluated the effects of alloying elements and impurities on radiation damage in Zr alloys. They found that cavity formation was more rapid during electron than during neutron irradiation. Griffiths (1988) reviewed the microstructure evolution in Zr alloys during irradiation. This review concludes that cavities form at temperatures between 350 and 500°C.

The cavities formed in Zr alloys during irradiation are commonly associated with intermetallic precipitates. Neutron irradiation of these intermetallic precipitates generates He gas helps to support the cavity. The cavities formed during creep also tend to be associated with intermetallic precipitates. The cavities produced during irradiation may contribute toward cavitation during post-irradiation creep and impact the strain achievable before fracture. A mechanism for this phenomenon involving bubble sweeping to grain boundaries by dislocation motion during post-irradiation creep has been described by Beere (1983).

An example of advanced cavitation in the cross section of an H.B. Robinson SNF Zry-4 cladding specimen after irradiation to 30 GWd/MTU and tensile tested at 371°C is shown in Figure 11 (Bauer and Lowry 1978). Cavity growth and consequential cavity-to-cavity linking are apparent.

Bai et al. (1994) show that for hydrogen contents below the ductile brittle transition temperature (DBTT), ductile fracture in Zry-4 involves nucleation, growth, and coalescence of voids. Hydrides are the privileged sites for cavity formation. After the voids initiate, their behavior can be described by existing ductile fracture theories. Their experimental investigations at 20 and at 350°C show fracture by the coalescence of voids (Figure 12). This mode of fracture is consistent with that predicted by the CSFM fracture maps at these conditions of temperature. To show the similarity of the fracture appearance for Zry-4 after fracture by grain boundary cavitation with the appearance of fracture by grain boundary cavitation in stainless steel, test results from Angeliu and Was (1994) are shown in Figure 13.

In addition to fracture by grain boundary cavitation, cavities also form in Zr alloys at the ends of hydrides (Puls 1988). An example of fracture from voids formed at hydrides in Zry-2 is shown in Figure 14.

Burton (1983) describes the effect of temperature and stress on the Zry-2 and Zry-4 boundaries separating fracture by creep cavitation from transgranular fracture. His results are in nominal agreement with the boundary defined by the CSFM fracture map.

Corso and Queeney (1981) investigated the crack growth process in Zry-4 at 315, 370, and 430°C. They found that porosity coalescence is a factor in the Zry-4 crack growth process.

Bocek and Hoffmann (1984) illustrate the effect of creep cavitation on the strain rate for Zircaloy-4 at 800°C. This is near the high temperature boundary between creep cavitation and transgranular fracture for Zry-4 on the CSFM fracture map.

These and numerous other experimental and theoretical publications for fracture mechanisms in Zr alloys clearly show that dismissal of the grain boundary cavitation as the potential failure mechanism during cask storage of SNF by ERPI (Pescatore and Cowgill 1994) and by BFS is inconsistent with a broad published, experimental and theoretical database. Creep tests designed to show the operability and role of cavitation

as a failure mode in SNF cladding under dry storage conditions may be required to support modeling of this mechanism. The approach taken in the CSFM method was to model grain boundary cavitation by normalizing the model to creep rupture data. Microstructural data to support detailed micromechanics approach were not available. The development of a fundamental understanding of the critical parameters based on test data is recommended

According to Wisner and Adamson (1996) strength and ductility of irradiated Zry are not affected by corrosion-induced hydrides at levels up to ~400 PPM. However, there are considerable data showing significant reductions in uniform and burst strains for higher hydride levels [See Section 3, Assessment of 1% Strain Limit].

2.4 Monkman-Grant Correlation for Zry-4

BFS indicated that a methodology employing a Monkman-Grant constant may be applicable for correlation of strain limits for high burnup SNF cladding. However, they concluded that data were insufficient to employ this method at this time. PNNL concurs that the Monkman-Grant approach may become a useful tool provided sufficient data become available.

2.5 Comparison of Spilker/BFS and CSFM Creep Predictions

The CSFM creep methodology (Chin and Gilbert 1989) is based on strain rate and fracture results from many investigations with Zr and Zr alloys. The results were compared with deformation and fracture maps for numerous metals and alloys and found to provide reasonable agreement over a wide range of temperature, stress, and temperature conditions. However, the data were limited to a burnup range < 45 GWd/MTU. It was found that most SNF could be stored in the mapped regions in which deformation was controlled by grain boundary sliding and failure was controlled by cavitation.

Comparison of the temperature dependence (Figure 15) and stress dependence (Figure 16) for the CSFM model and the Spilker et al. equation show similar complex behavior. The primary creep rate for the Spilker equation is calculated at 10,000 hours. The temperature and stress dependencies are similar to those predicted by the deformation maps of the CSFM methodology and the stress dependence described by Schaffler-Le Pichon et al. (1997) for unirradiated Zry-4. Figure 5 in Schaffler-Le Pichon et al. (1997) shows stress dependencies that are similar for irradiated Zry-4 at different burnup levels, but the transitions in slope are shifted to higher stress with increasing burnup level. The transitions in slope represent boundaries separating controlling mechanisms on the deformation maps. The boundaries shift with microstructural conditions. These data substantiate that more than one creep mechanism is operative depending on the stress and temperature.

The Spilker et al. equation and the CSFM methodology also generate similar strain profiles under similar conditions of a declining cask storage temperature. A comparison

is shown in Figure 17. In Figure 17, the temperature and stress transients are for a 5-cycle Zion Rod with the BFS cooling curve for 9.1-year old SNF during cask storage. This example is presented in Figure 4-17 in WCAP-15168. The Romieser creep data are also presented in WCA:-15168. Conservatisms built into the CSFM methodology to avoid approaching the threshold for failure are described in PNNL-6189. These conservatisms included: 1) no credit for creep rate reduction by irradiation and 2) a reduction of failure time (failure strain) by a factor of 10 with conservatively slow recovery by thermal annealing of cold work.

The CSFM cumulative damage fraction[1] and/or Spilker strain fraction are plotted as a function of maximum storage temperature in Figures 18, 19, and 20. These calculations are based on BFS peak cladding and peak rod average gas temperature cooling curves provided in Figure 4-16 of WCAP-15168. The peak rod average gas temperature decay is used to calculate the stress decay. The initial plenum temperature decay is assumed to be proportional to the assumed maximum temperature. The CSFM predicted storage temperature limits are provided in Figure 18 based two failure criteria -- the CSFM cumulative damage fraction and the BFS 1% strain limit. The CSFM damage fraction predicts a higher peak storage temperature (353°C) than the 1% strain limit (343°C). The CSFM and Spilker predicted peak cladding storage temperatures for different creep reduction factors between 1 to 10 are provided in Figure 20 assuming a failure criterion of cumulative damage fraction for CSFM and the BFS 1% strain limit for Spilker. These results show that the Spilker/BFS 1% strain limit combination predicts lower peak storage limits than the CSFM methodology if both methods use the same creep reduction factor. The results of these analyses are summarized in Table 2.

Table 2. Comparison of Temperature Limits for BFS and CSFM Creep Methods With 1%-Strain or Cumulative-Damage Failure Criteria

Method	BFS	BFS	BFS	CSFM
Creep Reduction Factor	10	2	1	1
1% Strain Limit	375°C	344°C	328°C	343°C
100% Damage*	387°C	363°C	353°C	353°C

*100% damage corresponds to the failure criteria in Levy et al. (1987).

Calculations summarized in Table 2 and in Figure 21 indicate that the conservatism of the BFS/Spilker/2 correlation is comparable to the CSFM method for stresses above 80 MPa, which is the lower limit of applicability for the Spilker equation.

Based on the review by PNNL of the BFS methodology, it is recommended that the BFS methodology may be accepted to determine dry storage temperature limits for SNF with burnup levels up to 60 GWd/MTU providing that: 1) the assumed strain limit is no more

[1] The cumulative damage fraction is the sum of the creep damage accumulated during each computational increment of temperature and stress. Failure is predicted as the damage fraction reaches 1.0.

than 1%, 2) the creep reduction factor is no more than two (2) and 3) the thickness of the water-side oxide is no more than 70 μm.

The acceptability of the high 60 GWd/MTU burnup is based on the post irradiation creep results for increasing neutron fluence that show the effect of irradiation displacement damage on the creep properties saturate at a burnup of ~45 GWd/MTU (Schaffler-Le Pichon et al. (1997). The acceptability of oxide thickness up to 70 μm is consistent with the findings of Wisner and Adamson (1996) that the strength and ductility of irradiated Zry are not affected by corrosion-induced hydrides at levels up to ~400 PPM. Thicker oxides are not accepted because of reported significant reductions in uniform tensile and burst strains.

3.0 Assessment of the 1% Strain Limit

Failure is defined by BFS as attainment of 1% uniform creep strain using the Spilker et. al. (1997) equation as modified by BFS with a creep reduction factor of 10. The creep reduction factor of 10 is based on normalizing the Spilker creep correlation, which bounds commercial cladding such as manufactured by Westinghouse or Sandvik (Limback and Andersson 1996) to the highly creep resistant FRG-2 cladding that is not bounding. BFS provides no description of the failure mechanism. However, BFS does provide results from short term tensile and burst tests to failure on irradiated cladding with a wide range of burnups up to 55 GWd/MTU (Tables 3-1 and 3-2 of WCAP-15168), short term creep tests at 350 and 400° C for unirradiated Zry-4 uniformly hydrided to 1040 ppm (Bouffioux and Ruppa 1999), and irradiated Zry-4 with hydride levels up to 3000 ppm (Peehs 1998). The mechanical burst tests in WCAP-15168 (Tables 3.1 and 3.2) on high burnup cladding includes only a very small amount of data for high burnup cladding with high values of cladding oxide thicknesses (>70 μm) and high average hydride levels (>450 ppm). The small amount of data that did exhibit high cladding hydrides demonstrated uniform strains <1% at fracture when the average hydrogen levels exceeded 450 to 500 ppm in the cladding. Some of this data does show uniform strains >1% but a large portion shows uniform strains <1%.

The Bouffioux and Ruppa data from unirradiated Zry-4 hydrided to 1040 ppm appears to contradict proprietary data available to the NRC that shows uniform cladding burst strains ≤1% when a hydride enriched (> 1000 ppm) rim is introduced on unirradiated Zry-4. The average hydrogen concentration for these Zry-4 specimens was ≥ 500 ppm when the uniform burst strains were ≤1%. As presented by BFS, Figure 11 from Peehs (1998) indicates that burst tests for irradiated Zry-4 with hydrogen contents exceeding 3,000 ppm exceed 1% (1 to 5%) strain. The strain scale is compressed and difficult to read. Figure 11 in Peehs et al. also implies, without supporting evidence, that higher strain values would be expected for lower stress values. These data appear to contradict the tensile and burst strain data from Tables 3-1 and 3-2 of WCAP-15168 and recent data from Garde et al. (1996).

Based on the above information it appears that cladding uniform strains are above 1% when average cladding hydride levels are somewhere below 400 to 500 ppm. Similarly, Wisner and Adamson (1996) have concluded that the strength and ductility of irradiated Zry are not affected by corrosion-induced hydrides at levels up to ~400 ppm. In addition the CSFM methodology of creep by grain boundary sliding provides a theoretical basis to expect cladding uniform strains greater than 1%. However, there are some data showing significant reductions in uniform and total strains for higher hydride levels.

Recent mechanical test data (tensile, ring, and burst tests) have been performed on SNF cladding irradiated in Calvert Cliffs up to local burnups greater than 60 GWd/MTU (Garde et al. 1996). Generally, the burst test specimens show the lowest cladding strains. These tensile and burst tests demonstrate that high burnup cladding with average hydrogen levels that exceed 450 ppm generally exhibit less than 1% uniform strain and there are very low uniform strains (<0.5%) when average hydrogen levels exceed 700 ppm.

BFS has also submitted additional proprietary burst strain data from fuel rod cladding with oxide thicknesses between 40 to 100 μm. These data demonstrate that cladding uniform strains drops significantly below 1% and total strains drop significantly below 1.5%, respectively, when oxide thicknesses equal 75μm and above at temperatures between 300 and 350°C. These data further suggest that cladding with oxide thicknesses of 75 μm will have a high probability of some spalling and the existence of hydride blisters at the spalling location. These results contradict the results from Garde et al. (1996) that did not show oxide spalling until oxide thicknesses exceeded 100 μm. These proprietary data further suggest that the heavily hydrided blisters (with local hydrogen contents between 1080 to 2000 ppm) are embrittled, lead to cracking in the blister, and are the source of the low observed ductilities. The burst strain data of irradiated cladding from Garde et. al. (1996), in Tables 3-1 and 3-2 of WCAP-15168, and the new BFS proprietary data appear to contradict the data from Peehs (1998). Based on the former references above and from Wisner and Adamson (1996), it is concluded that a 1% strain limit is conservative for low burnup fuel, i.e., < 45 GWd/MTU, but it is non-conservative for high burnup fuel with oxide thicknesses greater than 70 to 75 μm. Therefore, the 1% strain limit is not recommended for application to high burnup fuel with greater than 70 to 75 μm of oxide thickness.

Increased fuel burnup, in general, results in an increase in cladding oxide thickness. Recent high burnup fuel has demonstrated that oxide thicknesses near or above 100 μm (Chung et al. 1996, Van Swam et al. 1994) can be achieved at rod average burnups above 55 GWd/MTU. High oxide thicknesses impact cladding behavior because it consumes Zr metal reducing cladding thickness and more importantly results in a hydride enriched rim (~ 1100 to 2000 ppm in hydrogen) at the metal surface. This hydride-enriched rim appears to be quite brittle with oxide thicknesses of 70 to 75 μm at temperatures between room temperature and 350° C. The embrittled rim can be fairly thick or a thick blister can exist below a point where the oxide spalls off the cladding. The thick rim or blister is observed in cladding with oxide thicknesses above 70 to 75 μm. This hydride rim/blister results in crack initiation in the rim and low overall cladding ductility when the cladding

is subjected to short-term burst testing (Garde et al. 1996 and in Tables 3-1 and 3-2 of WCAP-15168). The burst tests are prototypic of the loading stresses due to rod pressures as experienced in dry storage with the exception of the short duration of the burst tests. The cladding ductility is near or below 1% uniform cladding strain when the average hydrogen content exceeds 450 to 600 ppm. It is difficult to estimate the exact hydrogen level at which the ductility falls below 1% uniform strain because of the lack of mechanical testing data from high burnup cladding with high corrosion and the variability in the existing data. The current hypothesis for the reduced ductility is due to the hydrides in the rim being crack or cavitation initiating points that lowers the overall strength and ductility of the cladding.

BFS was questioned about high oxide thicknesses in high burnup spent nuclear fuel (SNF) rods and the impact on the 1% uniform strain limit. BFS responded that only a small population of high burnup fuel has experienced oxide thickness greater than 50 μm and referenced oxide measurements from high burnup fuel discharged in the early 1980s. In addition, BFS has hypothesized that long term creep such as is the case for the SNF in dry cask storage will result in higher cladding strains and ductilities than observed for the short term tensile and burst tests. BFS has also referred to one short-term ring test by Garde et al. (1996) that demonstrated greater than 2% uniform strain with an oxide thickness of 102 μm (670 ppm hydrogen) that they claim demonstrates large strain capability with high oxide thicknesses

PNNL has reviewed these BFS responses and concludes that the BFS hypothesis that long term creep in zirconium alloys will result in greater ductility than observed in the short term mechanical tests can not be confirmed. This is because there are currently no long term creep tests on high burnup spent fuel cladding with oxide thicknesses greater than 20 μm. In relation to BFS's reference to the high burnup fuel discharged in the early 1980s including a number of lead test assemblies that typically had less than 50 μm of oxide thickness, it is noted that the observed low cladding oxidation in these fuel rods is because they were irradiated for seven to eight years at low powers. Current plants are operating with 18 and 24 month cycles, and discharging a significant amount of fuel with only two cycles of operation that have achieved rod average burnups in the mid-50 GWd/MTU range, while the discharged three-cycle fuel achieves rod burnups around 60 GWd/MTU. The two-cycle fuel is generally referred to as high duty fuel because it has achieved high burnups in only two cycles of operation (rod powers are relatively high) and has measured oxide thicknesses exceeding 70 μm. Therefore, current and future discharged fuel is expected to have a significant number of fuel rods with 70 μm of oxide thickness or greater.

PNNL has also reviewed the one ring test datum from Garde et al. (1966) referred to by BFS and notes that this test appears to be atypical of the results from the tensile and burst tests also presented in the Garde paper. For example, Garde presents results from a total of 5 burst and tensile specimens with hydride levels greater than 460 ppm and all but one of these specimens exhibited less than 1% uniform strain. In addition, the ring tests are not prototypical of the stress state of pressurized SNF cladding. These ring tests also have a bending load that further complicates the interpretation of these results to

pressurized cladding. Garde also notes that the burst tests result in lower ductilities than either the tensile or ring tests. Also noted above, the burst tests provide the most prototypical stress state for pressured SNF cladding.

The above short term tensile and burst tests suggests that the hydride rim may reduce strain capability resulting in cladding uniform strains less than 1% when average hydrogen levels exceed 450 to 500 ppm. Therefore, it is recommended that the NRC limit the level of hydrogen content for SNF cladding subjected to dry cask storage until long-term stress-creep tests can be performed on high burnup cladding with oxide thicknesses greater than 70 μm. Because hydrogen content in the cladding is not easily measured without destructive examination and cladding oxide thickness can be related to average hydrogen levels it is further recommended that oxide thickness be used to identify those SNF with average hydrogen levels greater than 450 ppm. This level of average hydrogen content corresponds to an oxide thickness of approximately 70 μm utilizing the recommended hydrogen pickup fraction of 0.15 from Lanning et. al. (1997).

It is also recommended that SNF with oxide levels greater than 80 μm can be put in dry cask storage and treated as damaged fuel.

4.0 Assessment of Maximum Rod Pressure

Rod pressure is the driving force for SNF failure during dry storage while cladding creep is the assumed failure mechanism by BFS. Therefore, the limiting rod pressures assumed by BFS are very important in the BFS analysis of SNF loading and temperature limits for dry cask storage.

BFS was questioned regarding justification and clarification of how BFS determined the limiting rod pressures used for SNF storage. BFS responded that they use the NRC-approved PAD 3.4 code and limiting normal operating power histories (peak operation rod) to predict best estimate maximum in-reactor rod pressures, and then add a small conservative adder in the rod pressures used for SNF dry storage. It is noted that these limiting in-reactor rod pressures for SNF are less than those calculated by Westinghouse for licensing analyses of fuel operating limits. Licensing analyses of fuel operating limits usually include the calculational uncertainties at a 95/95 level and also conservatively include several operating transients (e.g., Condition I and II transients) that are possible during normal operation. The BFS calculated limiting pressures do not include calculational uncertainties nor do they include possible Condition I and II transients. PNNL has performed an audit calculation with the NRC developed FRAPCON-3 fuel performance code (Lanning et al., 1997 a & b) similar to the one performed by BFS, i.e., best estimate prediction of rod pressure from a limiting rod power history. The FRAPCON-3 fuel performance code calculated significantly lower rod pressures of ~1700 psi without Condition I and II transients and ~ 2000 psi with Condition I and II transients. This is compared to the conservative rod pressure of ~ 2250 psi used by BFS to determine their maximum cladding temperature limit for dry cask storage.. The FRAPCON-3 code predicted lower pressures because it is a recently developed state-of-

the-art code that uses the latest models and verified against the latest well-characterized high burnup fuel performance data. The PAD 3.4 was developed nearly 20 years ago and has been validated against only a limited amount of high burnup data that was not as well characterized as today's data. These limitations in the PAD code resulted in a code that tended to overpredict fission gas release and rod pressures. PNNL concludes that the limiting in-reactor pressure assumed by BFS are conservative, but most likely not at the 95/95 confidence level required for in-reactor licensing analyses. The in-reactor bounding pressures are generally between 2500 to 3000 psi depending on the fuel design and the fuel vendor. The exact level of conservatism in the BFS calculated limiting pressure is difficult to determine.

BFS further responded that they utilize a conservative methodology to estimate SNF rod pressure in dry storage; however, this methodology includes BFS accounting for the lower temperatures at the ends of the rod where the fuel rod plenum resides. PNNL has performed an audit calculation with the FRAPCON-3 code. The FRAPCON-3 code used an axial temperature profile of a spent fuel rod in the BFS dry storage cask calculated using the COBRA-SF code developed by PNNL for calculating temperatures in storage casks. The COBRA-SF analysis of cladding temperatures was similar to that performed by BFS. The FRAPCON-3 code predicted lower rod pressures for dry cask storage than those predicted with the BFS methodology. These audit analyses demonstrated that the BFS methodology for calculating SNF rod pressures for dry cask storage from in-reactor rod pressures is conservative.

5.0 Major Issues Identified

5.1 Variability in Creep for different Lots of Zr Alloys

Unirradiated creep data presented by BFS show ~10x variability in creep strain/rate. Creep is sensitive to grain size, composition, texture, and other material parameters. The development of the Spilker equation was based on a lot of Zry-4 with the highest creep rate (Type 1 material), while the Zry-4 used for the FRG-2 cladding was the most creep resistant of cladding tested to date. The creep resistance of the Sandvik Zry-4 lot tested by Limback and Andersson (1996) is similar to that for the Type 1 Zry-4 used by Spilker et al. to model the creep behavior. Consequently, the BFS analysis is not conservative for Sandvik cladding.

Post irradiation creep data by Einziger and Kohli (1984) shows a large variability in post-irradiation creep strains for several Turkey Point SNF rods. For the same time periods the large variability in strain is consistent with the variability in the FRG-2 creep strains for the same time period. The variability is exaggerated by the proximity to the onset of creep following a period for relaxation of the internal stresses. It takes several hundred hours or more for the strains generated by the applied stress during a creep test to become dominant over the internal strain fields established by the intergranular internal stresses. Internal stresses are generated by the irradiation growth in the anisotropic structure.

These internal intergranular stresses are also the stress fields under which the cavities may be generated.

The implication of these results is that the Spilker equation with a creep reduction factor of 1.0 bounds all published creep data for Zry-4 that were reviewed, including irradiated Zircaloy. However, the margin was not large. The creep reduction factor for Type I cladding was 1.0 for data at 10,000 hours for a temperature of 375°C and stresses of 80, 100, and 120 MPa. The creep reduction factor for Sandvik cladding at 385°C and 80 MPa was ~1.3. A creep reduction factor of 2 with the Spilker equation bounds the CSFM temperature limits (see Table 2 and Section 2.6). Therefore, the use of a creep reduction factor of not more than 1 or 2 bounds published creep results for SNF fuel cladding.

5.2 Embrittlement of Hydride Enriched Rim for Cladding with High Corrosion

The impact of the brittle hydride rim on cladding crack penetration and cladding degradation during storage, retrieval and handling after storage is unknown. Annealing of irradiated cladding during cask drying may provide a more uniform hydride distribution and anneal irradiation damage such that the cladding more nearly resembles that with the much-improved mechanical properties as tested by Bouffioux and Rupa (1999). Feasibility for annealing without excessive clad creep and radial reorientation of hydrides is required. Ballooning may interfere with post-storage handling or rod consolidation. Also radial hydride reorientation, which increases cladding embrittlement and reduces toughness, needs to be prevented. The effect of annealing on hydride resolution during cask drying and subsequent hydride formation as the fuel cools needs to be investigated. Therefore, there are no technical bases to apply either the BFS or the CSFM methodologies to SNF with severely hydrided cladding.

5.3 Early BWR Fuel Rods with Nodular Corrosion

BWR cladding fabricated more than 8 to 10 years ago were more susceptible to a large amount of nodular corrosion resulting in hydride blisters and possible loss of ductility. The degree of nodular corrosion (and loss of ductility) varied from plant to plant (depending on operation and water chemistry) and also between fuel vendors.

5.4 Summary of Issues

- A non-conservative feature of the BFS/Spilker equation is that it describes only transient creep. The creep rate is predicted to decrease during cask storage not only because of the decreasing pressure (hoop stress) and temperature associated with the decreasing decay heat, but also because the model fails to transition from saturated-transient to steady-state creep. Creep data and mechanistic creep models clearly show that for SNF dry storage conditions the transient creep stage saturates below the 1% strain limit used by BFS. Therefore the creep strains may be higher than predicted by the BFS/Spilker correlation. This issue could become more serious if the BFS/Spilker correlation were to be used with a fracture strain limit higher than 1%.

- The BFS/Spilker equation with a factor of 10 creep reduction is normalized to FRG-2 test cladding. This cladding is significantly more creep resistant than Sandvik, Westinghouse, and Framatome cladding.

- The temperatures, stresses, and times that BFS applied to Big Rock Point SNF cladding for dry storage extends beyond the applicable ranges for temperatures (100 to 400°C), stresses (80 to 150 MPa), and times (10,000 hours) specified by Spilker et al. (1997). Extraordinarily high values of allowable temperature resulted from BFS calculations for Big Rock Point SNF. These high temperatures were at least partially due to implementation of the irrational creep reduction factor of 10.

- The behavior of the hydrides in heavily oxidized SNF cladding during cask drying and subsequent cooling under stress during storage has not been determined.

- There is a reduction in strain capability of heavily-oxidized cladding based on fast tensile and burst tests. The reduction in creep strain capability of heavily-oxidized SNF cladding and its impact on fracture mechanisms for dry cask storage has not been determined.

- The behavior of heavily oxidized and hydrided SNF cladding during post storage retrieval and handling has not been determined.

- High temperatures encountered during short-term drying operations may anneal SNF cladding, dissolve hydride precipitates, and result in excessive cladding strain. The strain estimated by BSF for one drying sequence was 1.6%. The effect of high temperatures during cask drying may impact analyses of SNF cladding temperature limits with either the BFS/Spilker or CSFM models.

6.0 Conclusions

- For external oxide thickness <70 μm, the BFS/Spilker method with a creep reduction factor of two (2) and a cladding strain limit of 1% is applicable to a rod-average burnup of 60 GWd/MTU.

- The temperature limit for SNF with cladding oxide thicknesses between 70 and 80 μm shall be determined consistent with the above condition, except that 50% of the SNF shall be considered as failed. All SNF cladding with oxide thicknesses >80 μm shall be considered failed until acceptable conditions can be determined by reasonable analyses and testing.

- The BFS/Spilker creep correlation should not be used outside the range of applicable stresses (80 to 150 MPa), temperatures (100 to 400°C), and times (10,000 hours). An exception is made for the analyses for Big Rock Point SNF with a calculated stress of 70 MPa.

- The BFS 1% strain limit is conservative for SNF with cladding oxide thickness <70 μm. The cladding hydride content for non-canistered SNF is controlled by limiting the cladding oxide thickness to 70 μm. There are insufficient creep and other mechanical property data for SNF cladding with oxides thicker than 70 μm to determine the effect of the hydride rim on cladding creep fracture and fracture models. The nature of breaches for cladding with an oxide thickness is >70 μm has not been determined.

- PNNL concurs with the BFS arguments that cladding breaches during dry storage of SNF with <70 μm oxide thickness are expected to be micron-size pin holes or narrow cracks.

- Pin-hole or narrow-crack cladding breaches do not compromise confinement of SNF particles.

- PNNL performed an audit calculation of BFS pressure and stress calculations and conclude the values are either a best estimate or slightly conservative for a peak operating rod for currently available SNF. This audit is not applicable to new fuel designs or changes in plant operation such as new 24-month-long fuel cycles.

- The CSFM methodology, with use of the cumulative damage fraction, is applicable up to 50 μm of cladding oxide thickness. For oxide thicknesses greater than 50 μm, but less than 70 μm cladding failure, should be determined based on a 1% strain limit.

Recommendations

- Testing and analyses are required to determine the effects of low and high burnup cladding on the fracture properties that is cooling during storage and post-storage retrieval and shipping.

- Testing is required to determine the effect of the nonuniform hydrides on the creep and fracture for cladding with an oxide thicker than 70 μm during storage and post storage retrieval and handling.

- Testing is required to determine the effect of cask drying operations on SNF cladding recovery, strain and stressed hydride re-precipitation behavior during dry storage and subsequent retrieval and handling operations.

- Testing and analyses are required to determine the limiting strain conditions during cask drying and storage to prevent failure of high burnup SNF cladding.

7.0 Recommendations for Additional Investigations

- Determine the effect of hydrides on creep-strain behavior for SNF cladding
- Determine the effect of defects on cumulative damage and fracture
- Determine the range of variability for creep resistance of cladding in SNF inventory
- Update the DATING Code to account for new:
  - creep and rupture data and mechanisms for Zry-4 and advanced Zr alloys
  - annealing results
  - hydride effects

8.0 Bibliography

Adamson, R. B., R. P. Tucker, and V. Fidleris. 1982. "High-Temperature Irradiation Growth in Zircaloy," ASTM STP 754, 208-234, Zirconium in the Nuclear Industry, Fifth Conference, American Society for Testing and Materials, West Conshohocken, Pennsylvania.

Andrade, E. N. da C. 1910. "On the Viscous Flow in Metals and Allied Phenomena," Proc. Roy. Soc. London, A:84:1.

Andrade, E. N. da C. 1914. Proc. Roy. Soc. London, A:90:329.

Angeliu, T. M. and G. S. Was. 1994. "Creep and Intergranular Cracking of Ni-Cr-Fe-C in 360°C Argon," Met. and Mater. Trans. A, 25A:1169-1183.

ASTM B353-95. 1995. Standard Specification for Wrought Zirconium and Zirconium Alloy Seamless and Welded Tubes for Nuclear Service (Except Nuclear Fuel Cladding), American Society for Testing and Materials, West Conshohocken, Pennsylvania.

ASTM B811-97. 1997. Standard Specification for Wrought Zirconium Alloy Seamless Tubes for Nuclear Reactor Fuel Cladding, West Conshohocken, Pennsylvania.

Bai, J. B., C Prioul, and D. Francois. 1994. "Hydride Embrittlement in ZIRCALOY-4 Plate: Part I. Influence of Microstructure on the Hydride Embrittlement in ZIRCALOY-4 at 20°C and 350°C," Met. and Mater. Trans. A, 25A:1185-1198, The Metallurgical Society of AIME.

Bauer, A. A. and L. M. Lowry. 1978. "Tensile Properties and Annealing Characteristics of HB Robinson Spent Fuel Cladding," Nuclear Technology, 41:359-372, American Nuclear Society, LaGrange Park, Illinois.

Beere, W. 1983. "Cavity Nucleation During Post-Irradiation Creep," J. Nucl. Mater., 113:228-2233, Elsevier Science Publishers, Amsterdam, North-Holland.

BFS: Koehr, J. J., G. R. Thomas, J. N. Iyer, and J. E. Hopf. 1999. Dry Storage of High Burnup Spent Nuclear Fuel, WCAP-15118, Westinghouse Energy Systems, San Jose, California (Proprietary Information, Westinghouse Class 2).

Bocek, M., P. Hofmann, and C. Petersen. 1977. "Superplasticity of Zircaloy-4," ASTM STP 633, 66-81, Zirconium in the Nuclear Industry, American Society for Testing and Materials, West Conshohocken, Pennsylvania.

Bocek, M. 1985. "High Temperature Tensile Creep, Creep Damage and Failure Under Superimposed Compressional Stress," J. Nucl. Mater., 131:267-279, Elsevier Science Publishers, Amsterdam, North-Holland.

Bocek and Hoffman. 1984. "The Influence of Cavitation Damage Upon High Temperature Creep Under Stationary and Non-Stationary Loading Conditions," J. Nucl. Mater. 125:7-18, Elsevier Science Publisher, Amsterdam, North-Holland.

Bouffioux, P. and N. Rupa. 1999. "Impact of Hydrogen Pick up on Plasticity and Creep of Unirradiated Zircaloy-4 Cladding Tubes," ASTM STP (to be published), Twelfth International Symposium on Zirconium in the Nuclear Industry, American Society for Testing and Materials, West Conshohocken, Pennsylvania.

Bredel, T., C. Cappelaere, R. Limon, G. Pinte, and P. Bouffioux. 1999. "Long Term Creep Behavior of Spent Fuel Cladding for Storage and Disposal," Symposium on Scientific Basis for Nuclear Waste Management XXIII- Cladding and Spent Fuel, Materials Research Society Fall Meeting, Boston, Massachusetts.

Burton, B. 1983. "Creep Fracture Processes in Zircaloy," J. Nucl. Mater., 113:172-178, Elsevier Science Publishers, Amsterdam, North-Holland.

Cheng, B., P. M. Gilmore, and H. H. Klepfer. 1996. "PWR Zircaloy Fuel Cladding Corrosion Performance, Mechanisms, and Modeling", Proceedings of the 11th International Symposium on Zirconium in the Nuclear Industry, Garmish-Parenbirchen, Germany, September 11-14, 1995, American Society for Testing and Materials, Philadelphia, Pennsylvania.

Chin, B. A., and E. R. Gilbert. 1989. "Prediction of Maximum Allowable Temperatures for Dry Storage of Zircaloy-Clad Spent Fuel in Inert Atmosphere." Nucl. Tech. 85:57-65, American Nuclear Society, LaGrange Park, Illinois.

Corso, U. M. and R. A. Queeney. 1981. "Sustained Load Crack Growth in Zircaloy-4 at Elevated Temperatures," Met. Trans. A, 12A:357-359, The Metallurgical Society of AIME.

Einziger, R.E. and R. Kohli. 1984. "Low-Temperature Rupture Behavior of Zircaloy-Clad Pressurized Water Reactor Spent Fuel Rods under Dry Storage Conditions," Nucl. Tech., 67:107-122, American Nuclear Society, LaGrange Park, Illinois.

Fidleris, V. 1979. "Primary Creep of Zircaloy-2 Under Irradiation," ASTM STP 681, 177-188, Zirconium in the Nuclear Industry (Fourth Conference), American Society for Testing and Materials, West Conshohocken, Pennsylvania.

Foster, JP. 1991. Thermal Creep of Stress Relief Annealed Zircaloy-4 Tubing, STC Report 91-1TE4-IMPRV-R1, Westinghouse Electric Corporation (Westinghouse Proprietary Class 2).

Garde, A.M., GP Smith, and R.C. Pirek. 1996. "Effects of Hydride Precipitate Location and Neutron Fluence on the Ductility of Irradiated Zircaloy-4," ASTM STP 1295, Zirconium in the Nuclear Industry: Eleventh International Symposium, 407-430, E.R. Bradley and G.P. Sabol, Eds, American Society for Testing and Materials.

Gilbert, R. W., K. Farrell, and C. E. Coleman. 1979. "Damage Structure in Zirconium Alloys Neutron Irradiated at 573 to 923K," J. Nucl. Mater., 84:137-148, Elsevier Science, Amsterdam, The Netherlands.

Griffiths, M., R. W. Gilbert, V. Fidleris, R. P. Tucker, and RB Adamson. 1987. "Neutron Damage in Zirconium Alloys Irradiated to 644 to 710K," J. Nucl. Mater., 150:159-168, Elsevier Science, Amsterdam, The Netherlands.

Griffiths, M., R. W. Gilbert, and C. E. Coleman. 1988. "Grain Boundary Sinks in Neutron-Irradiated Zr and Zr-Alloys," J. Nucl. Mater., 159:405-416, Elsevier Science, Amsterdam, The Netherlands.

Griffiths, M. 1988. "Review of Microstructure Evolution in Zirconium Alloys During Irradiation," J. Nucl. Mater., 159:159-16X, Elsevier Science, Amsterdam, The Netherlands.

Griffiths, M., D. Gilbon, C. Regnard, and C. Lemaignan. 1993. "HVEM Study of the Effects of Alloying Elements and Impurities on Radiation Damage in Zr-Alloys," J. Nucl. Mater., 205:273-283, Elsevier Science, Amsterdam, The Netherlands.

Griffiths, M, R. C. Styles, C. H. Woo, F. Phillipp, and W. Frank. 1994. "Study of Point Defect Mobilities in Zirconium During Electron Irradiation in a High-Voltage Electron Microscope," J. Nucl. Mater., 208:324-334, Elsevier Science, Amsterdam, The Netherlands.

Hayes, T. A., R. S. Rosen, M. E. Kassner, and K. S. Vecchio. 1999. "Analysis Of Dry Storage Temperature Limits For Zircaloy-Clad Spent Nuclear Fuel," Symposium on Scientific Basis for Nuclear Waste Management XXIII- Cladding and Spent Fuel, Materials Research Society Fall Meeting, Boston, Massachusetts.

Holt, R. A., R. W. Gilbert, and V. Fidleris. 1982. "Dislocation Substructure in Zirconium Alloys Irradiated in EBR-II," ASTM STP 782, 234-250, Eleventh Conference, American Society for Testing and Materials, West Conshohocken, Pennsylvania.

Hoppe, N. E. 1991. "Engineering Model for Zircaloy Creep and Growth," 1:201-209, International Topical Meeting on LWR Fuel Performance - Fuel for the 90's, American Nuclear Society, LaGrange Park, Illinois.

Kaspar, G., M. Peehs, and E. Steinberg. 1985. "Experimental Investigation of Post-Pile Creep of Zircaloy Cladding Tubes," Transactions of 8th International Conference on Creep in Reactor Technology, Vol. C-D:51-57, North Holland, Amsterdam.

Kearns, J. J., J. E. McCauley, and F. A. Nichols. 1976. "Effect of Alpha/Beta Phase Constitution on Superplasticity and Strength of Zircaloy-4," J. Nucl. Mater., 61:169-184, Elsevier Science, Amsterdam, The Netherlands.

Koehr, J. J., G. R. Thomas, J. N. Iyer, and J. E. Hopf. 1999. Dry Storage of High Burnup Spent Nuclear Fuel, WCAP-15168, Westinghouse Energy Systems, San Jose, California (Proprietary Publication).

Keusseyan, R., C. Hu and C. Li. 1979. "Creep Damage in Zircaloy-4 at LWR Temperatures," J. Nucl. Mater., 80:390-392, Elsevier Science, Amsterdam, The Netherlands.

Keusseyan and C. Y. Li. 1981. "Kinetics of Creep Cavity Nucleation in Zircaloy-2," J. of Metals, 33:63, AIME.

Lanning D. D., C. E. Beyer, and C. L. Painter. 1997a. *FRAPCON-3:* Modifications to Fuel Rod Material Properties and Performance Models for High Burnup Applications, NUREG/CR-6534, Volume 1 (PNNL-11513, Volume 1), Prepared for the U.S. Nuclear Regulatory Commission by Pacific Northwest National Laboratory, Richland, Washington.

Lanning, D. D., C. E. Beyer, and G. A. Berna. 1997b. *FRAPCON-3:* Integral Assessment, NUREG/CR-6534, Volume 3 (PNNL-11513, Volume 3), Prepared for the U.S. Nuclear Regulatory Commission by Pacific Northwest National Laboratory, Richland, Washington.

Limback, M and T Andersson. 1996. "A Model for Analysis of the Effect of Final Annealing on the In- and Out-of-Reactor Creep Behavior of Zircaloy Cladding," ASTM STP 1295, 449-468, Eleventh International Symposium on Zirconium in the Nuclear Industry, American Society for Testing and Materials, West Conshohocken, Pennsylvania.

Luthy, H., R. A. White, and O. D. Sherby. 1979. "Grain Boundary Sliding and Deformation Mechanism Maps," Materials Science and Engineering, 39:211-216, Elsevier Sequoia, The Netherlands.

Peehs, M., E. Steinberg, G. Kaspar, D. Jorde, and H. Schonfeld. 1983. "ZRY Post-Pile Creep: Experimental Procedure, Test Samples and First Results," IAEA - Seminar on Technical and Environmental Aspects of Spent Fuel Management, September 27-30, 1983, Madrid, Spain.

Peehs, M. 1998. "Assessment of Dry Storage Performance of Spent LWR Fuel Assemblies with Increasing Burn-Up," Co-ordinated Research Program (CRP) on Spent Fuel Performance Assessment and Research (SPAR), First RCM Held in Washington DC.

Pescatore, C. and M. Cowgill. 1994. Temperature Limit Determination for the Inert Dry Storage of Spent Nuclear Fuel, EPRI-TR-103949, Electric Power Research Institute, Palo Alto, California.

Prasad, N., G. Malakondaiah, K. Muraleedharan, and P. Rama Rao. 1988. "Creep of Zircaloy-2 at Low Stresses," J. Nucl. Mater., 158:30-41, North-Holland Publishing Co, Amsterdam, The Netherlands.

Puls, M. P. 1988. "The Influence of Hydride Size and Matrix Strength on Fracture Initiation at Hydrides in Zirconium Alloys," Met. Trans. A, 19A:1507-1522.

Ruano, O. A., A. K. Miller, and O. D. Sherby. 1981. "The Influence of Pipe Diffusion on the Creep of Fine-Grained Materials," Materials Science and Engineering, 51:9-16, Elsevier Sequoia, The Netherlands.

Schaffler-Le Pichon, I., P. Geyer, P. Delobelle, and P. Bouffioux. 1997. "Modeling of the Mechanical Behavior of Zircaloy-4 Cladding Tubes from Unirradiated State to High Burn-Up," 219-225, Proceedings of the 1997 International Topical Meeting on Light Water Reactor Fuel Performance, Portland, Oregon.

Shukla, S. V., C. Chandrashekharayya, R. N. Singh, R. Fotedar, R. Kishore, T. K. Sinha, and BP Kashyap. 1999. "Effect of Strain Rate and Test Temperature on Superplasiticty of a Zr-2.5 wt% Nb Alloy," J. Nucl. Mater., 273:130-138, North-Holland Publishing Co, Amsterdam, The Netherlands.

Spilker, H., M. Peehs, H. P. Dyck, G. Kaspar, and K. Nissen. 1997. "Spent LWR Fuel Dry Storage in Large Transport and Storage Casks after Extended Burnup," J. Nucl. Mater., 250:63-74, Elsevier Science, Amsterdam, The Netherlands.

Toscano, B. H., and M. Bocek. 1981. "Relationship Between Strain Rate, Strain to Failure and Lifetime," J. Nucl. Mater., 96:29-36, North-Holland Publishing Co, Amsterdam, The Netherlands.

Van Swam, L. F., F. Garzarolli and E. Steinberg, 1994. "Advanced PWR Cladding", Proceedings 1994 International Topical Meeting on Light Water Reactor Fuel Performance, West Palm Beach, Florida, April 17-21, 1994, American Nuclear Society.

Westerman, R. 1966. "Charging Zircaloy-2 with Hydrogen Beyond the Solubility Limit," J. Nucl. Mater., 18:31-38, North-Holland Publishing Co, Amsterdam, The Netherlands.

Wisner, S. B. and R. B. Adamson. 1996. "Combined Effects of Radiation Damage and Hydrides on the Ductility of Zircaloy-2," Enlarged Halden Program Group Meeting, Norway.

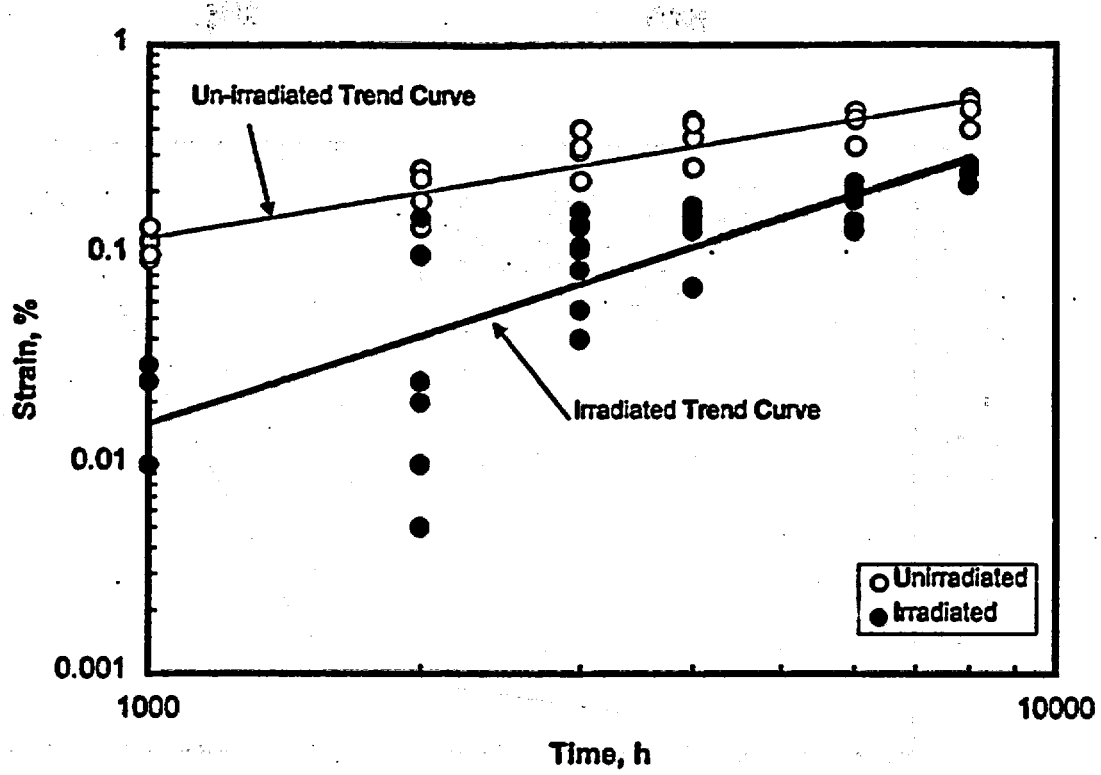

Figure 1. Evaluation of Time Exponents for Unirradiated and Irradiated FRG-2 Cladding Creep Strain at 395°C and 86 MPa

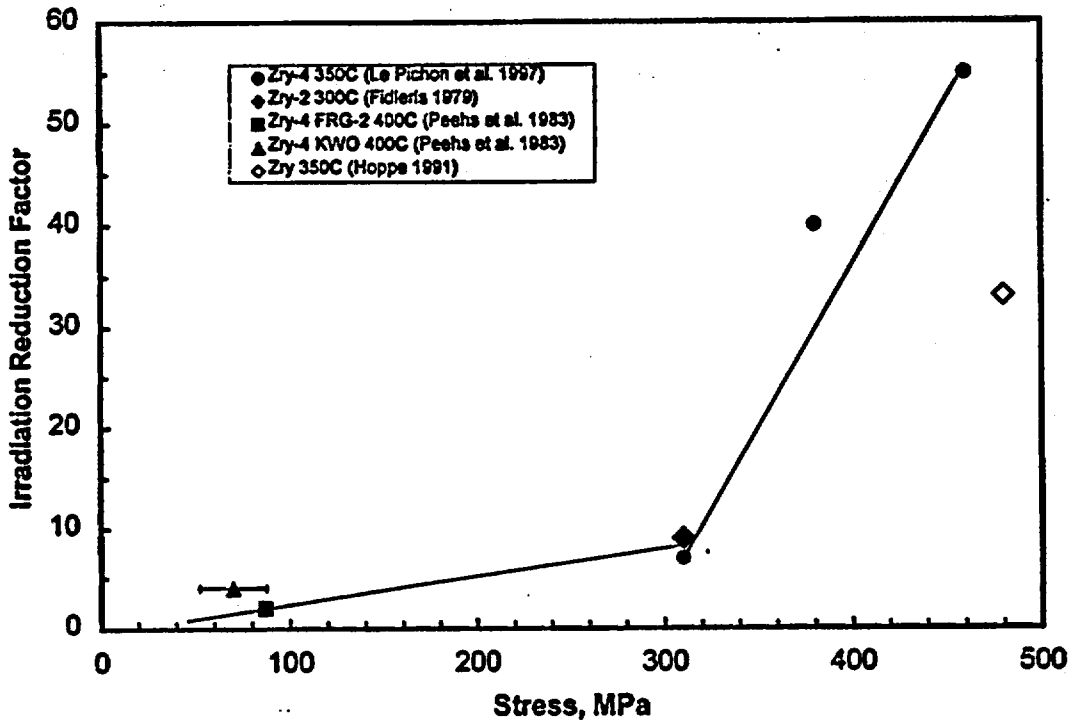

Figure 2. Effect of Stress on Creep Reduction Factor for Irradiated Zry-4

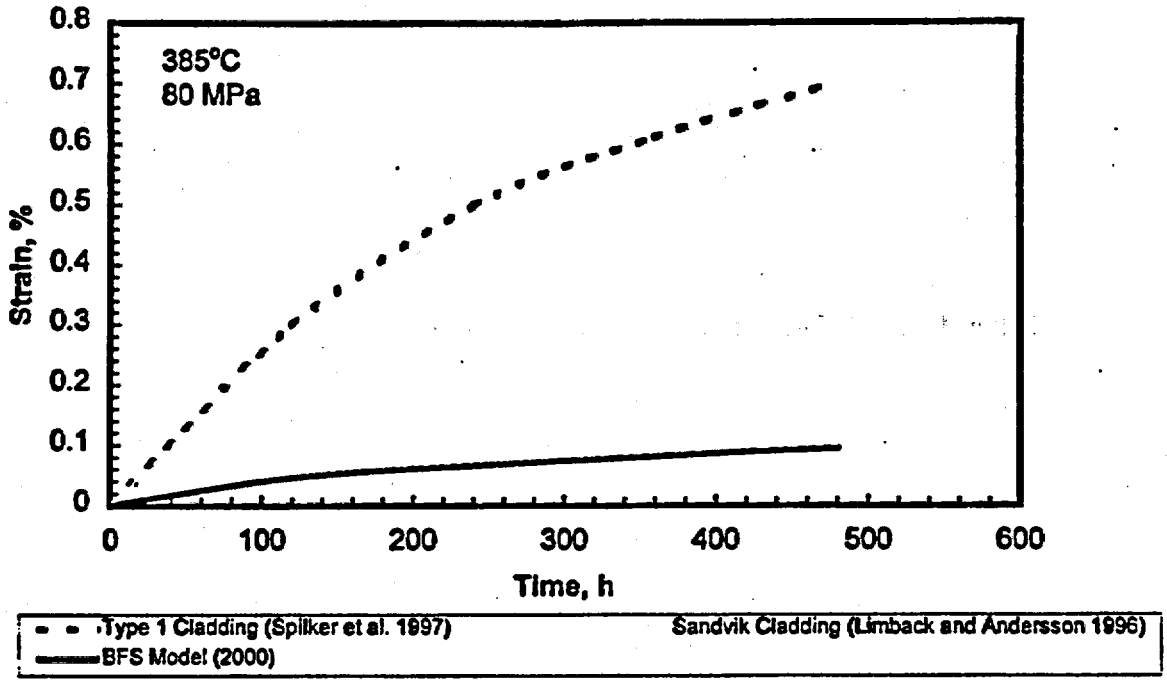

Figure 3. Comparison of Creep Strains for Type I Cladding with Creep for Sandvik Cladding

Figure 4. Deleted - Proprietary Information

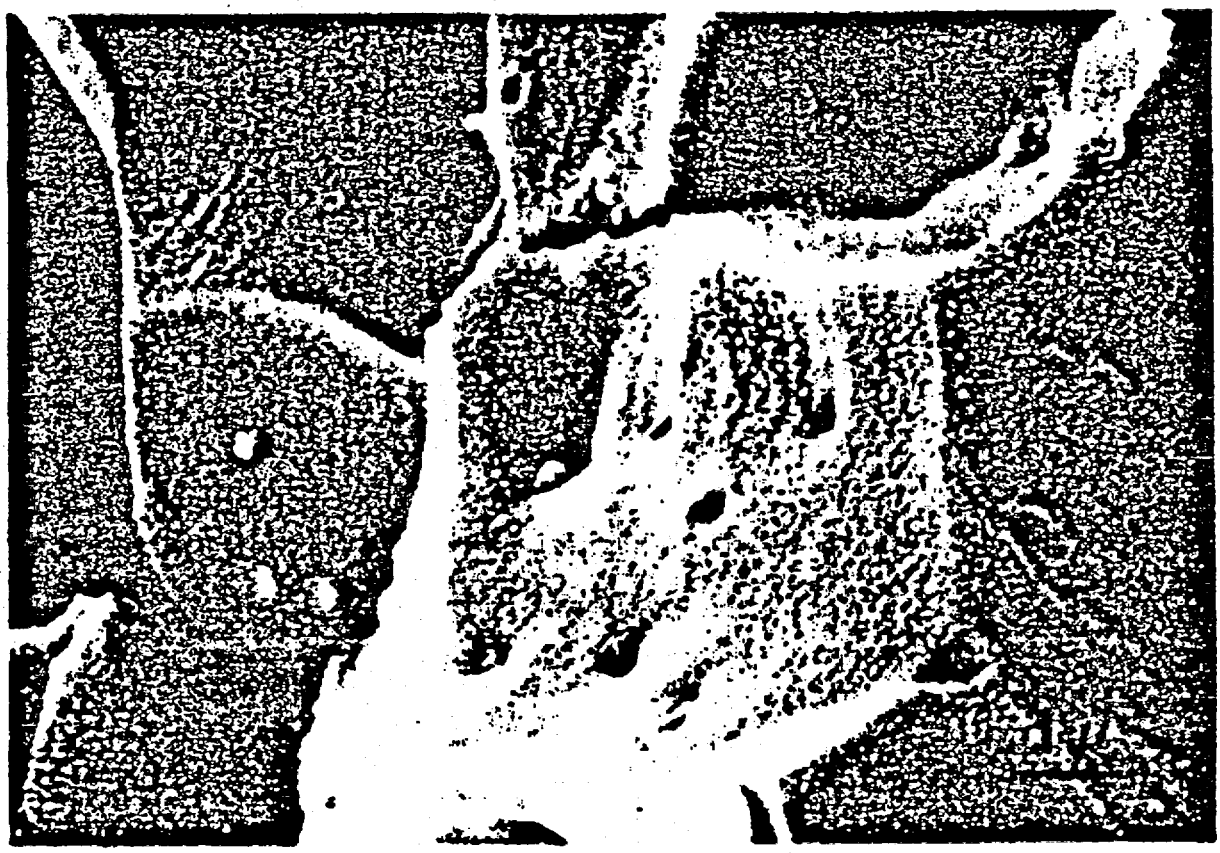

Figure 5. Scanning Electron Micrograph showing Cavities in Zry-4 Specimens Crept for 240 h to 3 % Strain at 375°C and 132 MPa. No cavities were found in unstrained specimens (Keusseyan et al. 1979). The number density of grain boundary cavities in Zry-2 specimens increased with increasing creep strain (Keusseyan and Li 1981).

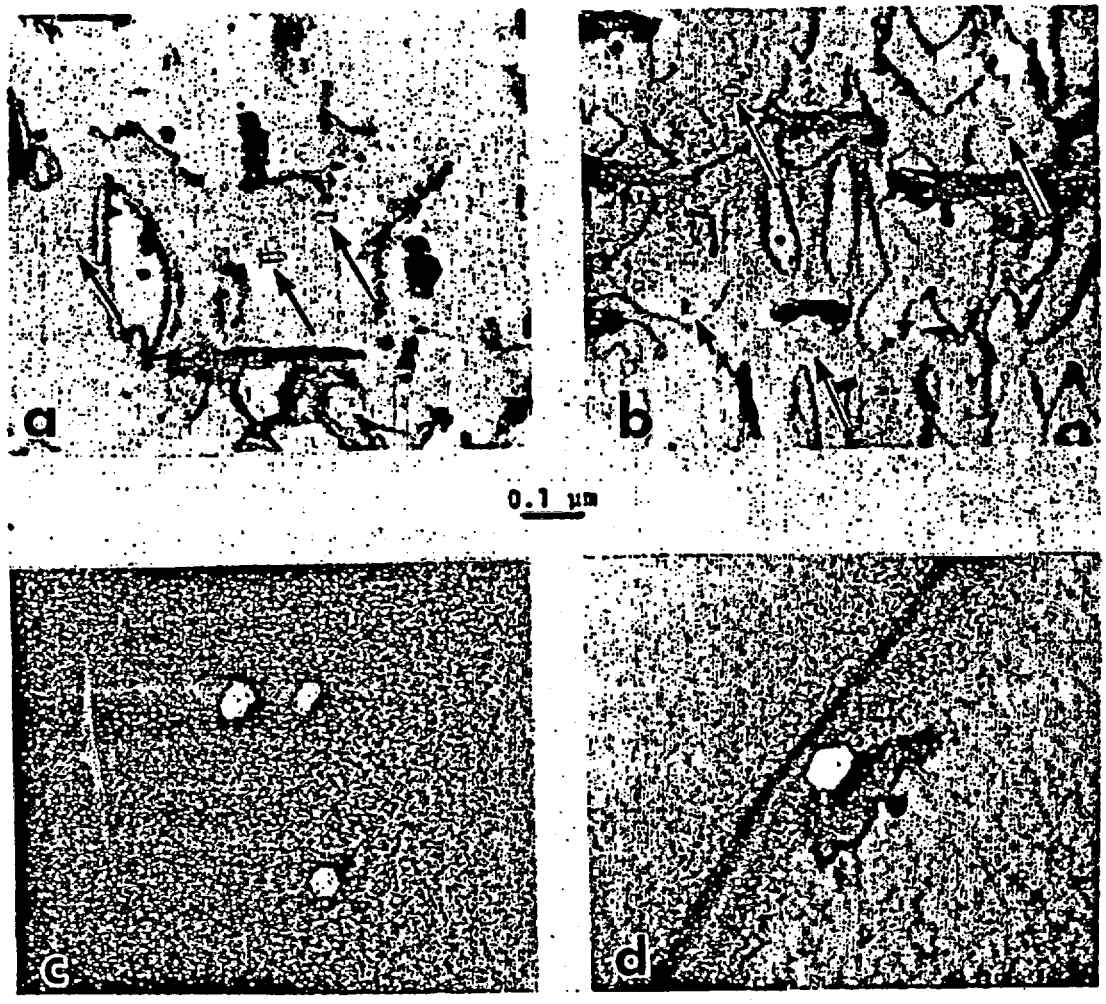

Figure 6. Radiation-Induced Cavities in Zr Alloys [ORR]

Annealed Zr; 400°C; 1.2 x 10^{21} n/cm^2 E>0.1 MeV
Annealed Zry-2; 400°C; 1.2 x 10^{21} n/cm^2 E>0.1 MeV
Annealed Zr-2.5 wt% Nb; 650°C; 0.7 x 10^{21} n/cm^2 E>0.1 MeV
Grain Boundary Cavity: same as c)

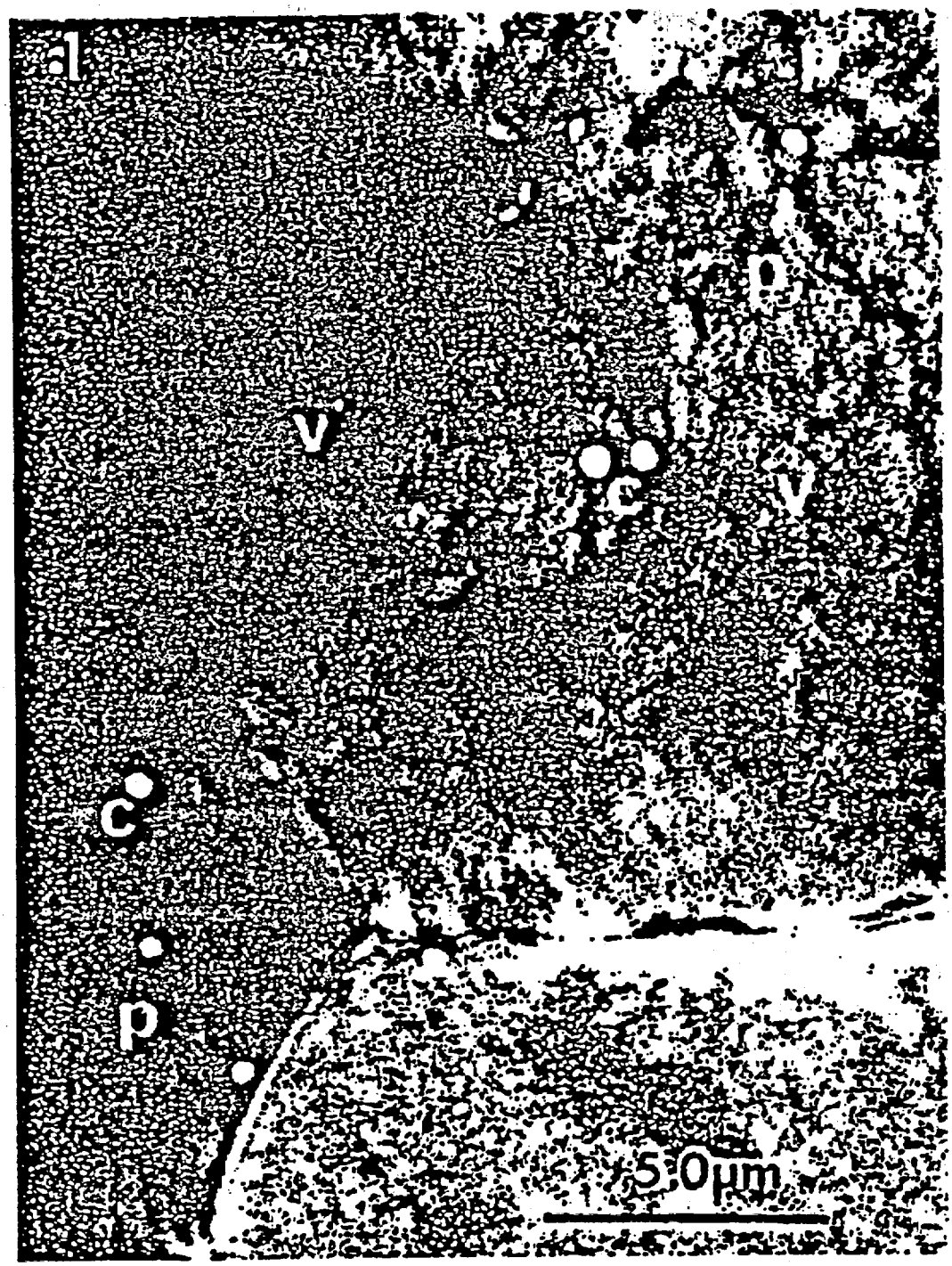

Figure 7. TEM Micrograph of Zry-4 Showing Voids "v" and Cavities "c" after Irradiation in EBR-II at 381C and 1.4 to 6.3 x 10^{21} n/cm2 E>1 MeV (Adamson et al. 1982)

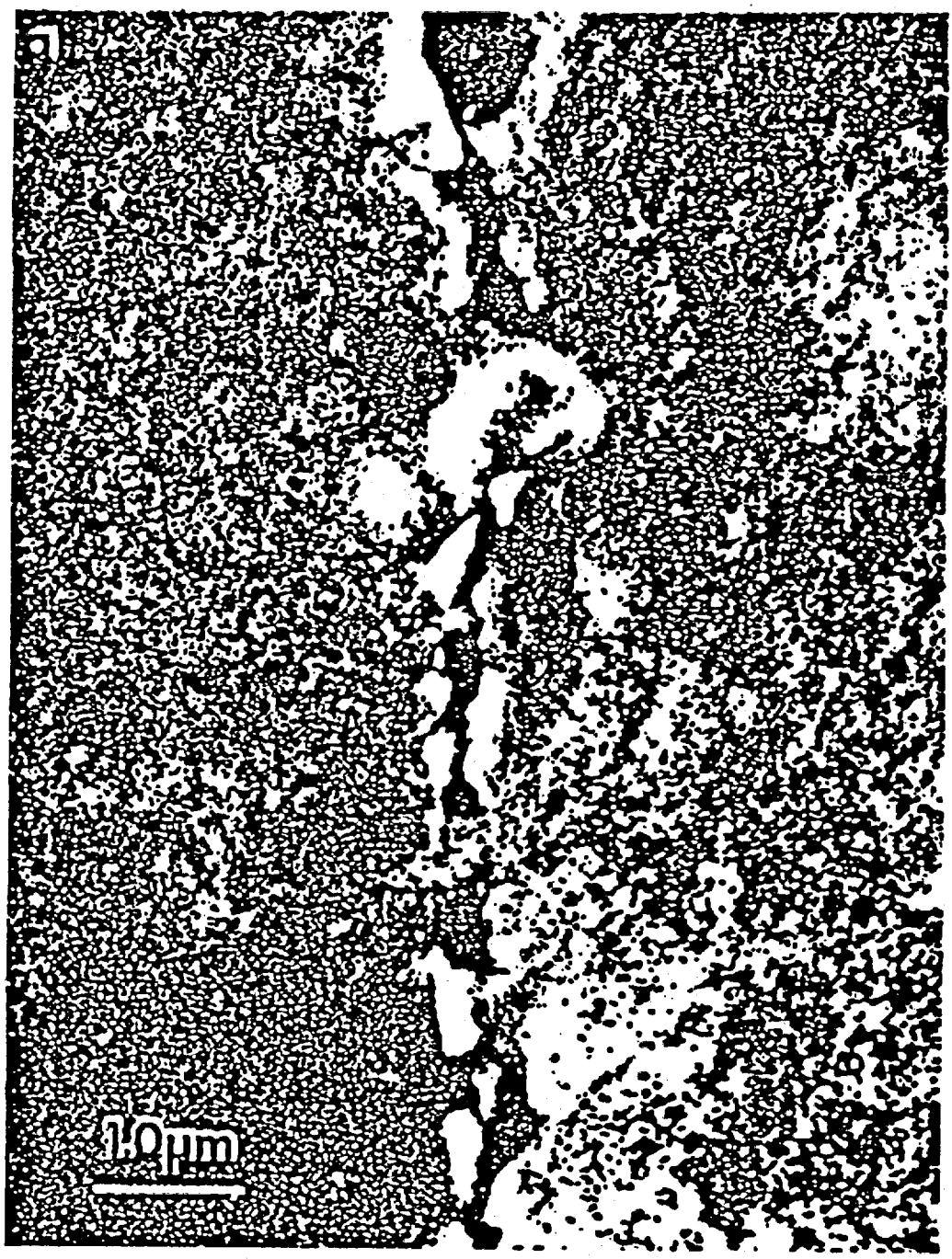

Figure 8. TEM Micrograph of Irradiated Zry-4 Showing Grain Boundary Cavitation after Irradiation in EBR-II at 381°C and 1.4 to 6.3 x 10^{21} n/cm^2 E>1 MeV (Adamson et al. 1982)

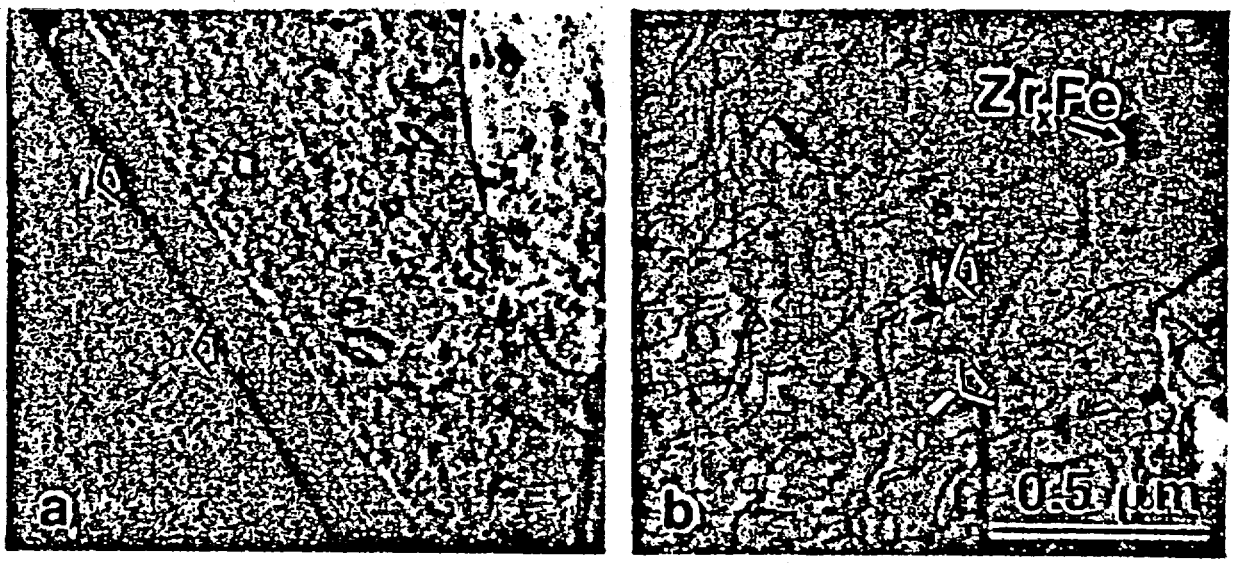

Figure 9. Cavities in Zr After Irradiation in EBR-II (Griffiths et al. 1987) at:
427°C, 1.08 x 10^{21} n/cm^2 E>1 MeV
437°C, 5.3 x 10^{21} n/cm^2 E>1 MeV

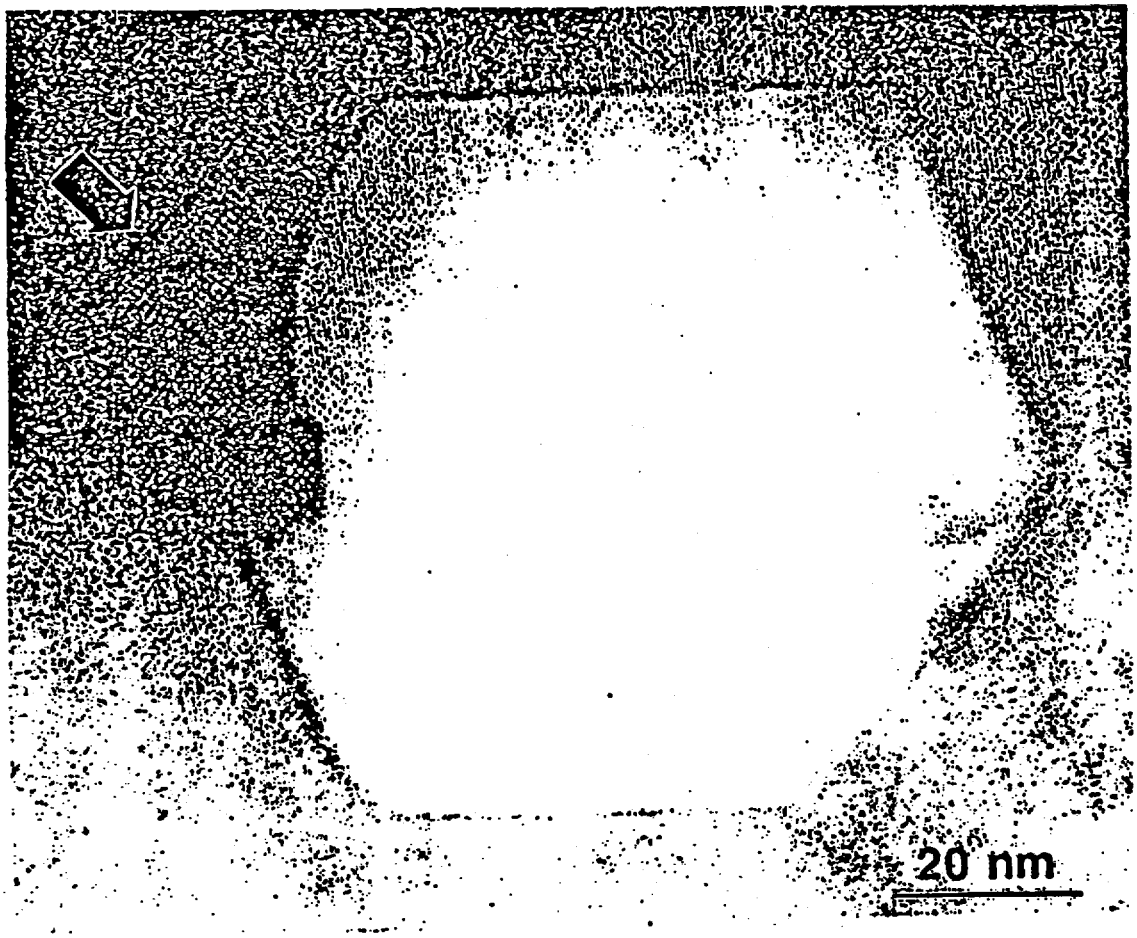

Figure 10. Cavity in Zr Irradiated in DFR at 452°C, 1.7 x 10^{21} n/cm^2 E>1 MeV (Griffiths et al. 1994)

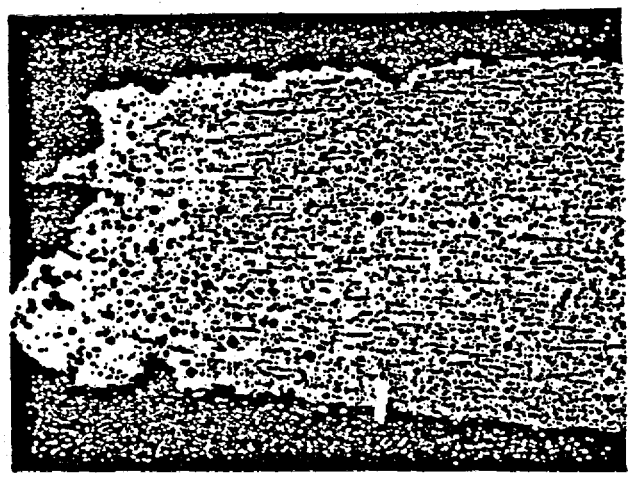

(a)

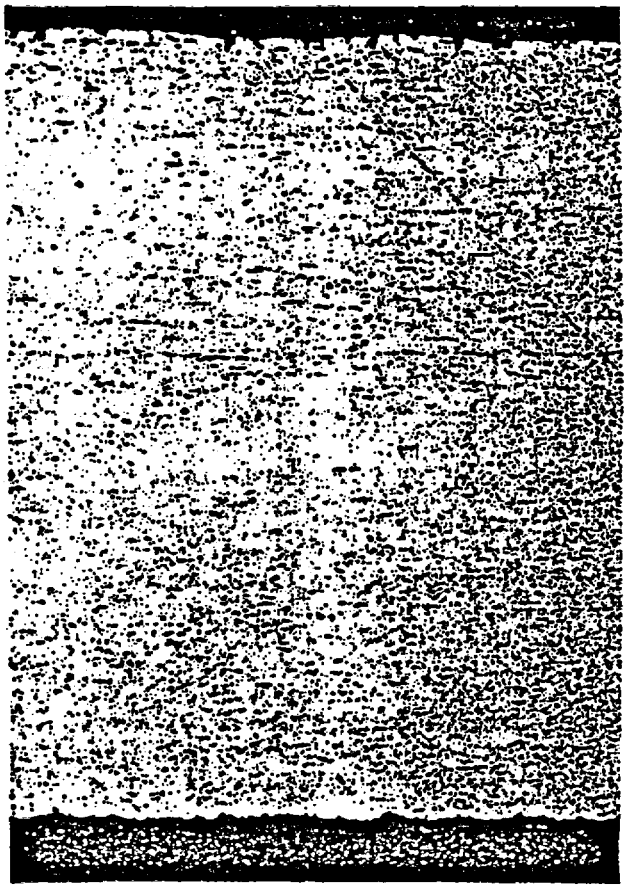

(b)

Figure 11. Tensile Test Fracture in 30 GWd/MTU H.B. Robinson Zry-4 Cladding by Cavitation (Bauer and Lowry 1978)

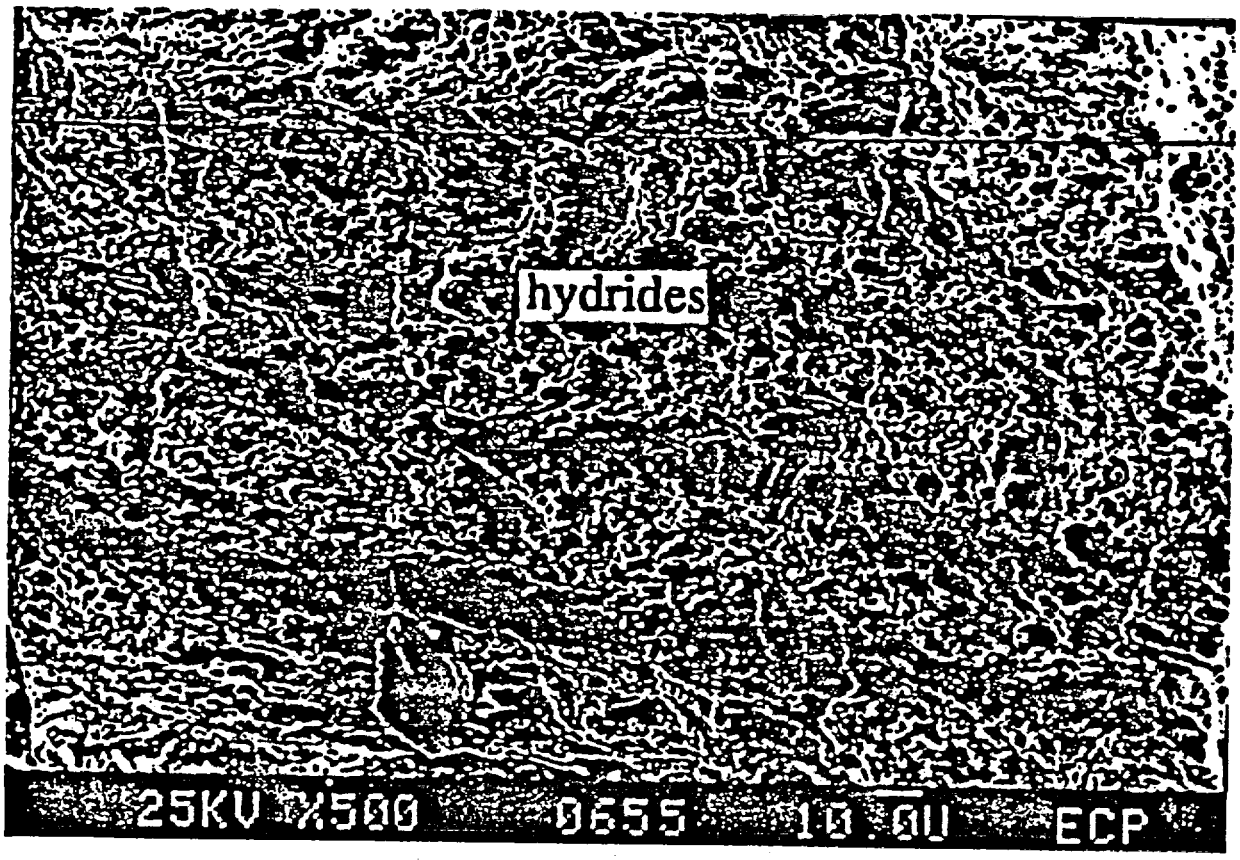

Figure 12. Fracture in Zry-4 by Nucleation, Growth, and Coalescence of Voids (Bai et al. 1994)

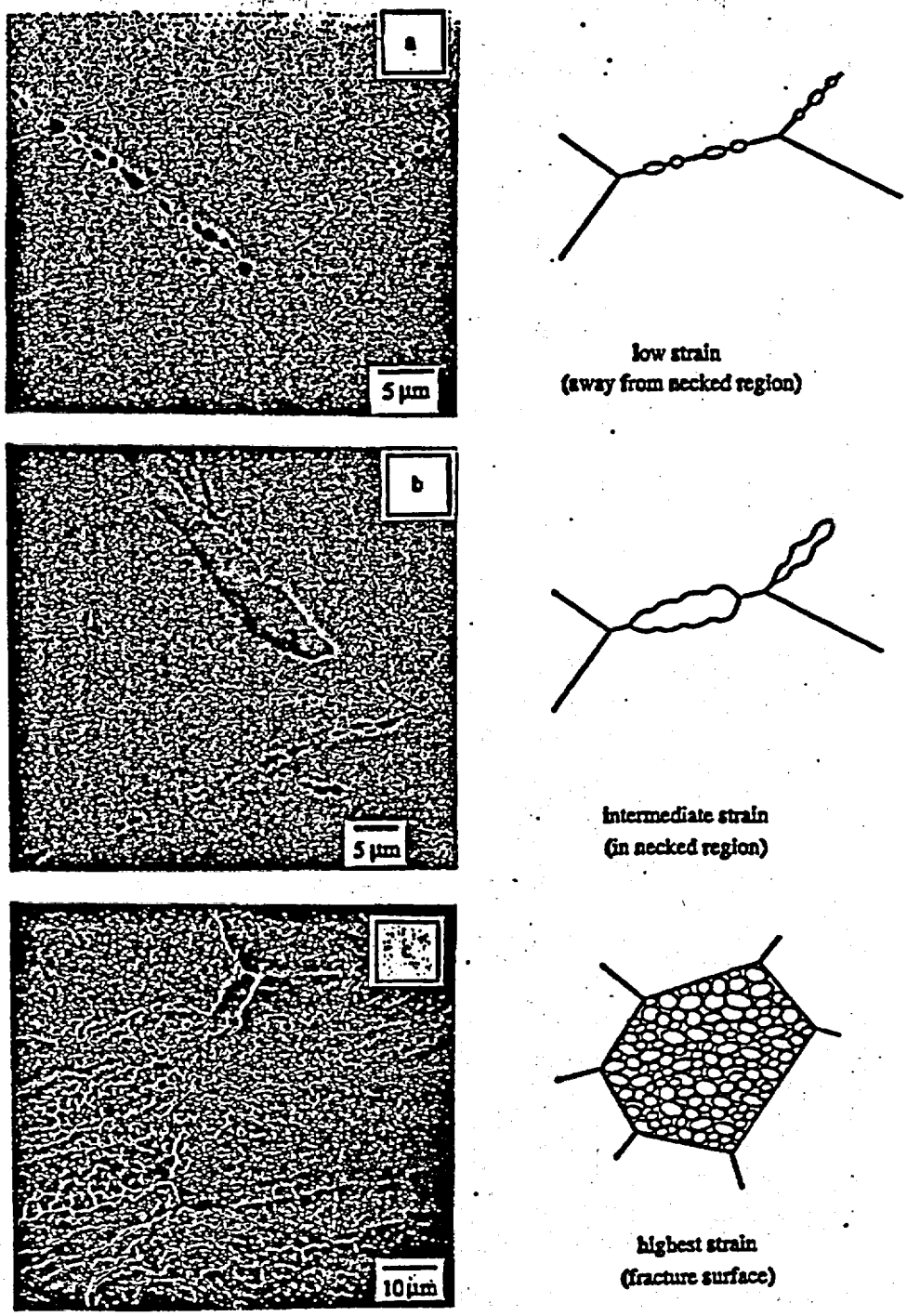

Figure 13. Fracture in Stainless Steel by Nucleation, Growth, and Coalescence of Voids (Angeliu and Was 1994)

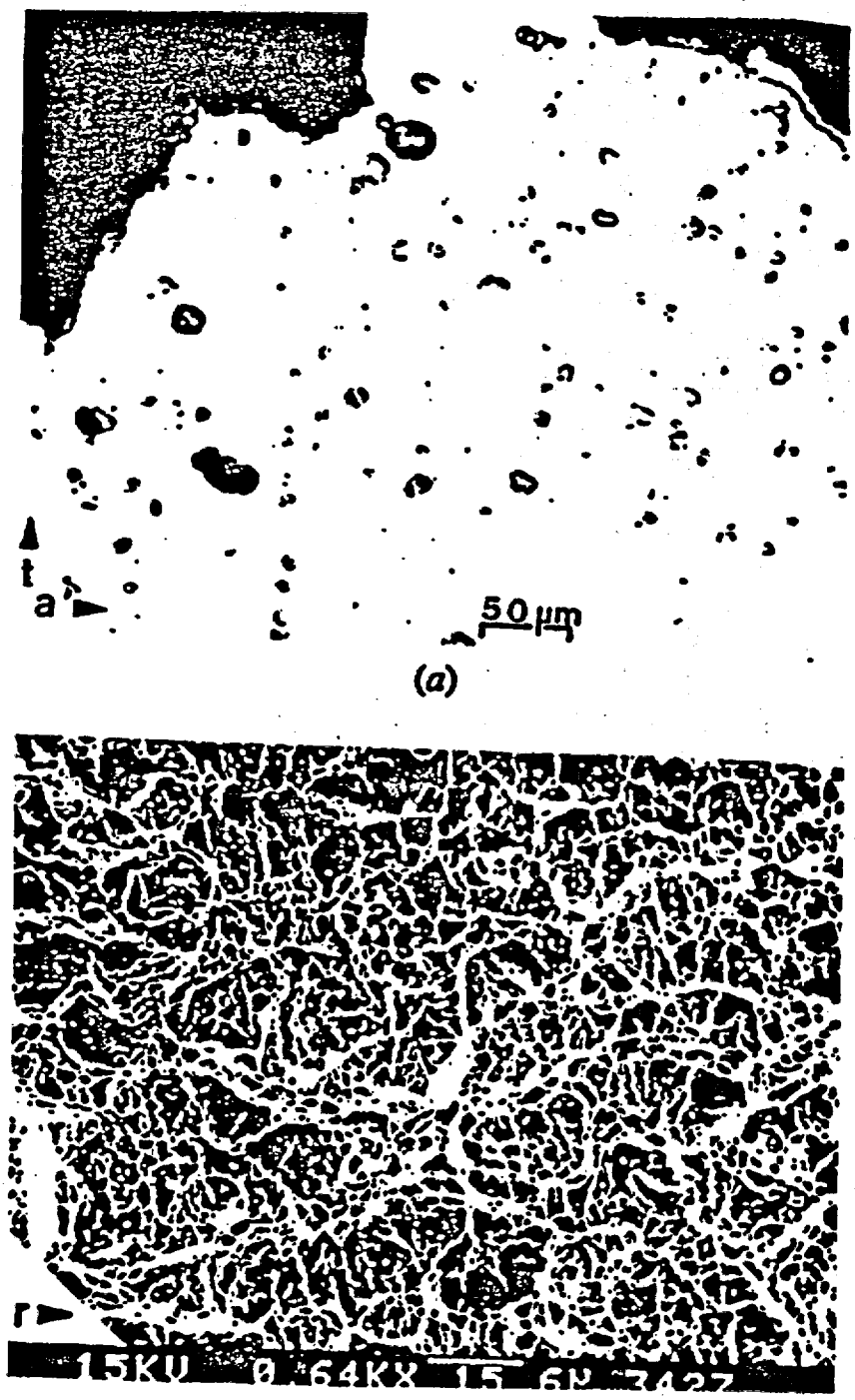

Figure 14. Fracture in Zry by Nucleation, Growth, and Coalescence of Voids (Puls 1998)

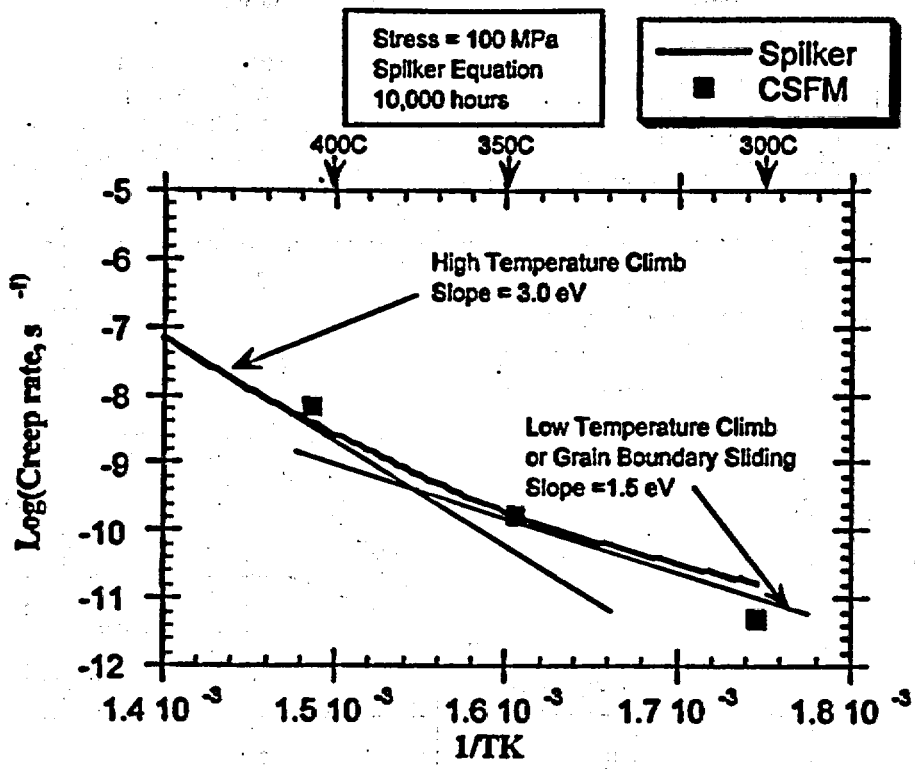

Figure 15. Comparison of the Temperature Dependence for the Spilker et al. (1997) Equation and the CSFM Methodology (Levy et al. 1987)

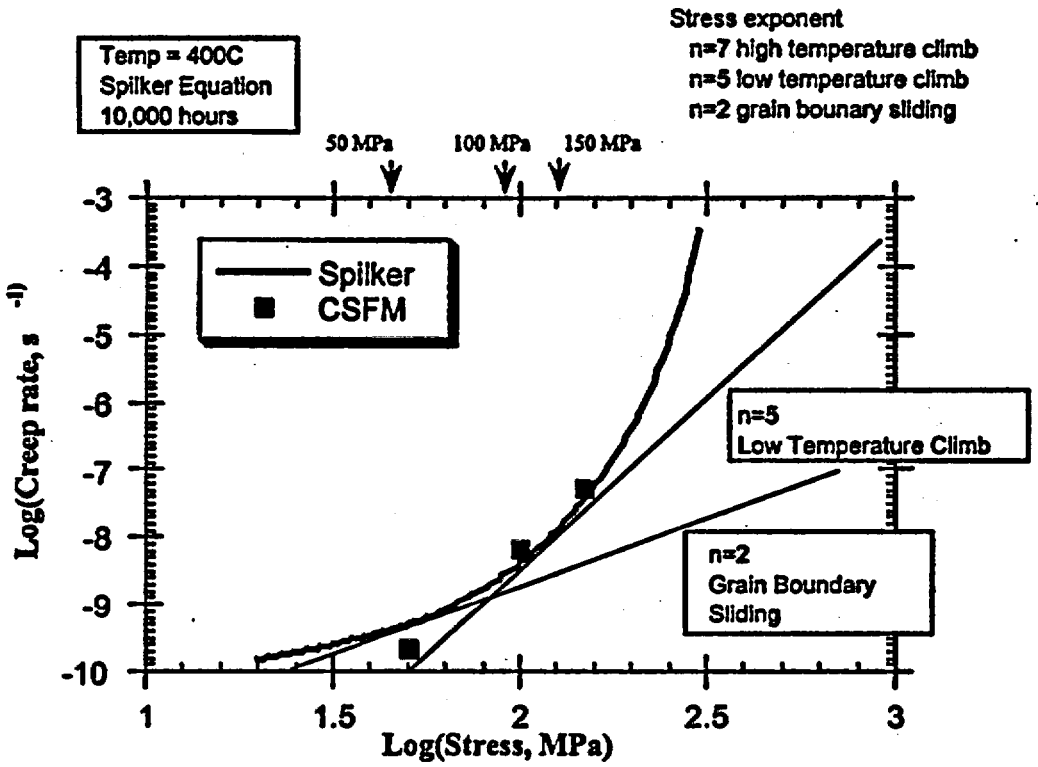

Figure 16. Comparison of the Stress Dependence for the Spilker et al. (1997) Equation and the CSFM Methodology (Levy et al. 1987)

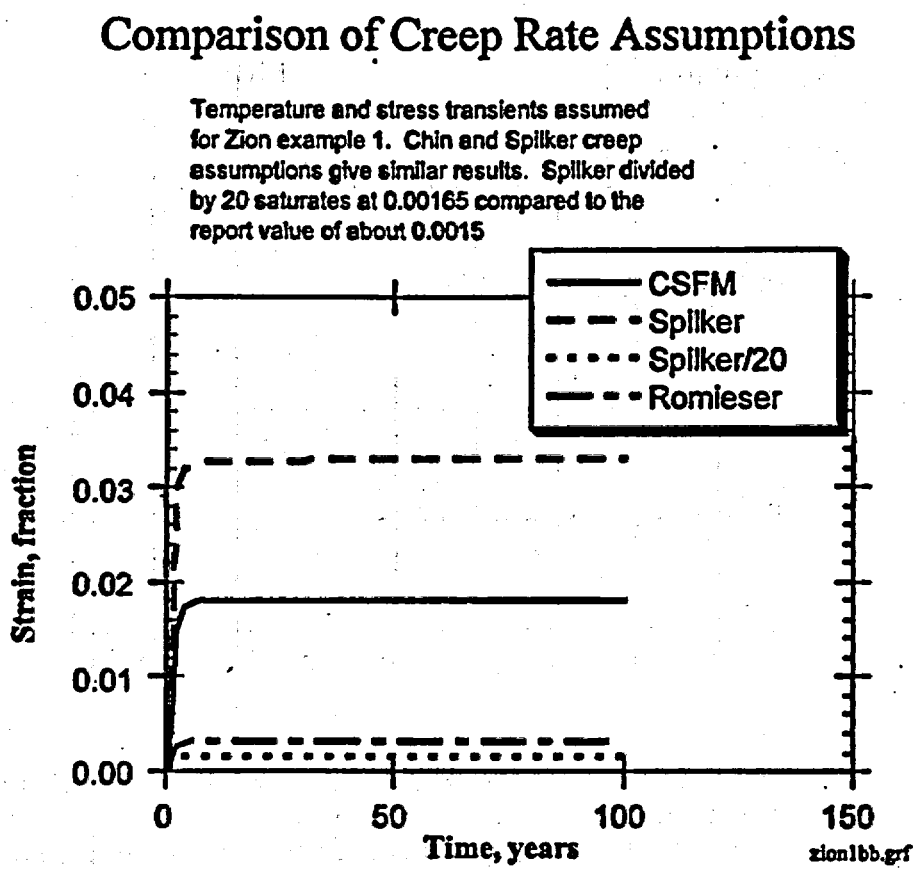

Figure 17. Comparison of Predicted Strain vs Time for the Spilker et al. (1997) Equation and the CSFM Methodology (Levy et al. 1987); Temperature and Stress Transients are for Zion Example 1 with the BFS Cooling Curves for 9.1-Year-Old SNF During Cask Storage

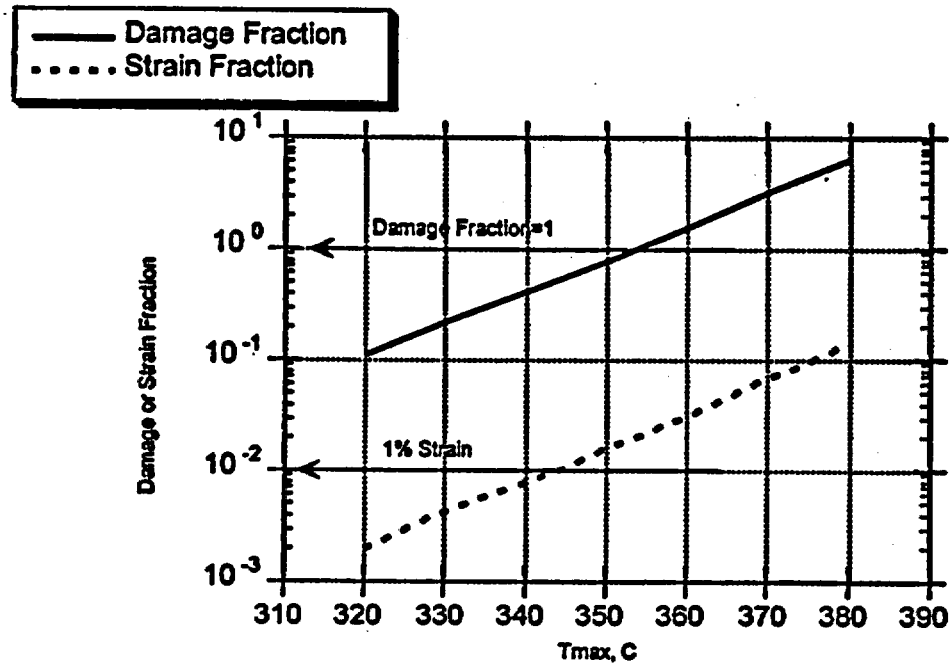

Figure 18. Comparison of Calculated Damage Fraction and Strain Fraction versus Initial Maximum Cladding Temperature with No Creep Reduction as Calculated by the CSFM Methodology for an Initial Cladding Stress of 122 MPa and the BFS Cooling Curves in Figure 4-16, page 4-31 from WCAP-15168

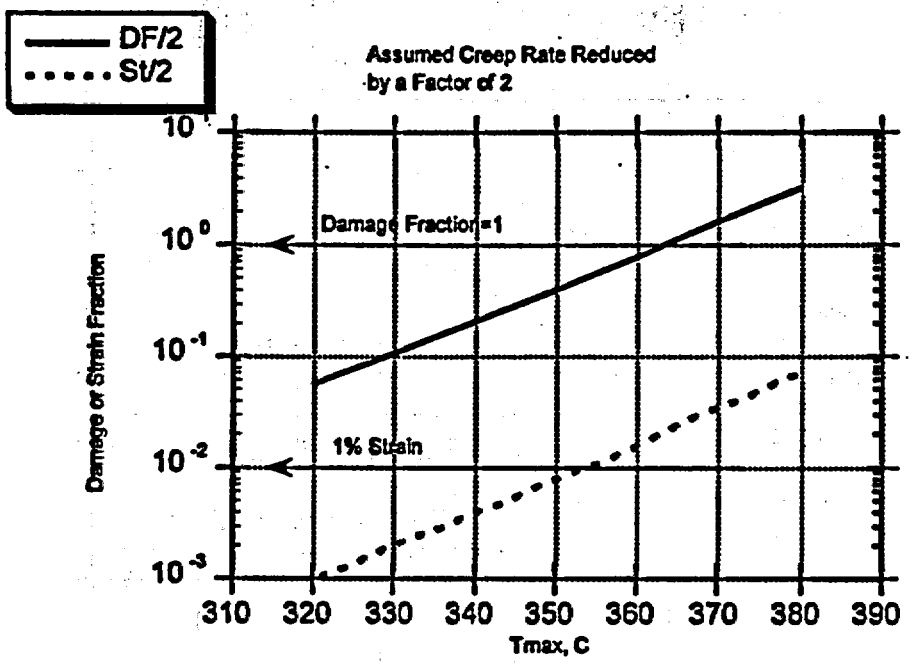

Figure 19. Comparison of Calculated Damage Fraction and Strain Fraction versus Initial Maximum Cladding Temperature with a 50% Creep Reduction Factor as Calculated by the CSFM Methodology for an Initial Cladding Stress of 122 MPa and the BFS Cooling Curves in Figure 4-16, page 4-31 from WCAP-15168

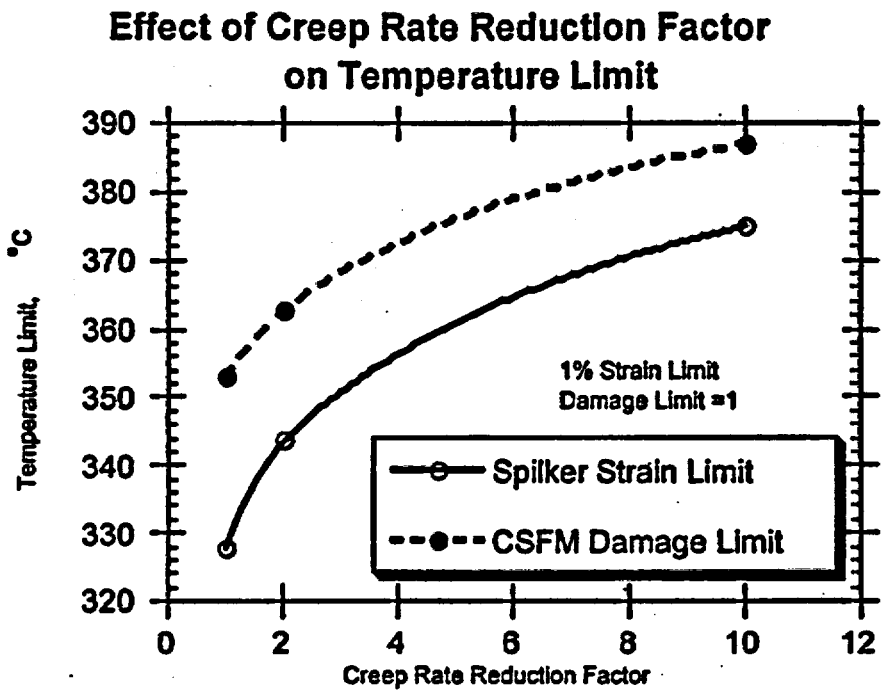

Figure 20. Effect of Creep Reduction Factor on Temperature Limits for BFS 1% Strain Limit Method and the CSFM Damage Limit Method

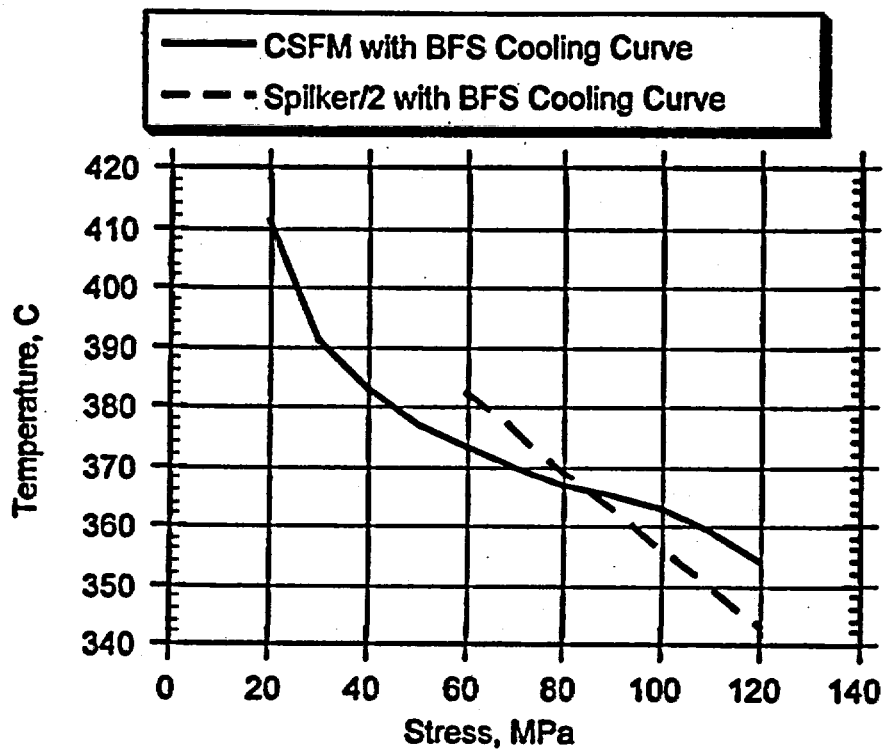

Figure 21. Effect of Stress on Temperature Limits Showing the BFS/Spilker/2 Correlation Is Conservative Compared to the CSFM Methodology for Stresses above 80 MPa. (Note: 80 MPa is the lower limit of applicability for the Spilker Equation.)